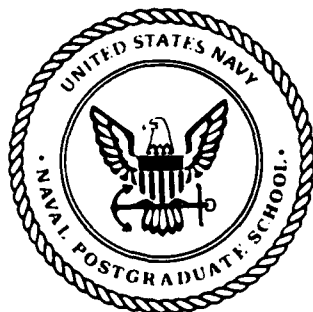


AD-A219 893

NAVAL POSTGRADUATE SCHOOL Monterey, California



THESIS

EXPERIMENTS ON LIQUID IMMERSION
NATURAL CONVECTION COOLING OF
LEADLESS CHIP CARRIERS MOUNTED ON
CERAMIC SUBSTRATE

by

Rufino A. Paje

September 1989

Thesis Advisor:

Yogendra Joshi

Approved for public release; distribution is unlimited

DTIC
ELECTE
MAR 29 1990
S B D

REPORT DOCUMENTATION PAGE				Form Approved OMB No 0704-0188	
1a REPORT SECURITY CLASSIFICATION UNCLASSIFIED			1b RESTRICTIVE MARKINGS		
2a SECURITY CLASSIFICATION AUTHORITY			3 DISTRIBUTION / AVAILABILITY OF REPORT		
2b DECLASSIFICATION / DOWNGRADING SCHEDULE					
4 PERFORMING ORGANIZATION REPORT NUMBER(S)			5 MONITORING ORGANIZATION REPORT NUMBER(S)		
6a NAME OF PERFORMING ORGANIZATION Naval Postgraduate School		6b OFFICE SYMBOL (If applicable)	7a NAME OF MONITORING ORGANIZATION Naval Postgraduate School		
6c ADDRESS (City, State, and ZIP Code) Monterey, California 93943-5000			7b ADDRESS (City, State, and ZIP Code) Monterey, California 93943-5000		
8a NAME OF FUNDING / SPONSORING ORGANIZATION		8b OFFICE SYMBOL (If applicable)	9 PROCUREMENT INSTRUMENT IDENTIFICATION NUMBER		
8c ADDRESS (City, State, and ZIP Code)			10 SOURCE OF FUNDING NUMBERS		
			PROGRAM ELEMENT NO	PROJECT NO	TASK NO
			WORK UNIT ACCESSION NO		
11 TITLE (Include Security Classification) EXPERIMENTS ON LIQUID IMMERSION NATURAL CONVECTION COOLING OF LEADLESS CHIP CARRIERS MOUNTED ON CERAMIC SUBSTRATE					
12 PERSONAL AUTHOR(S) RUFINO A. PAJE					
13a TYPE OF REPORT Master Thesis		13b TIME COVERED FROM _____ TO _____		14 DATE OF REPORT (Year, Month, Day) 1989, September	
15 PAGE COUNT 86					
16 SUPPLEMENTARY NOTATION The views expressed in this thesis are those of the author and do not reflect the position of the Department of Defense or the U.S. government.					
17 COSATI CODES			18 SUBJECT TERMS (Continue on reverse if necessary and identify by block number)		
FIELD	GROUP	SUB-GROUP	leadless chip carriers, liquid immersion		
			cooling natural convection		
19 ABSTRACT (Continue on reverse if necessary and identify by block number) An experimental investigation of natural convection heat transfer from a commercially available semiconductor device package is presented. The package was centrally mounted on a ceramic substrate. The package-substrate assembly formed one surface of a dielectric-filled cubical enclosure of aspect ratio one. The top surface of the enclosure was maintained at prescribed temperature. Surface temperature measurements were made at various locations on the substrate, the package lid, as well as the chip center. These measurements are reported for three dielectric fluids and three enclosure top surface temperatures, both with the substrate oriented horizontally as well as vertically. Heat transfer results are also expressed in non-dimensional form. The results indicate that the maximum input power without exceeding a chip junction temperature					
20 DISTRIBUTION / AVAILABILITY OF ABSTRACT <input checked="" type="checkbox"/> UNCLASSIFIED UNLIMITED <input type="checkbox"/> SAME AS RPT <input type="checkbox"/> DTIC USERS			21 ABSTRACT SECURITY CLASSIFICATION Unclassified		
22a NAME OF RESPONSIBLE INDIVIDUAL Yogendra Jushi			22b TELEPHONE (Include Area Code) (408) 646-2033		22c OFFICE SYMBOL 69J1

Unclassified

SECURITY CLASSIFICATION OF THIS PAGE (When Data Entered)

of 80°C is 2.58 watts with FC-75 as the cooling fluid and the upper boundary maintained at 15°C. This is significantly larger than the maximum of 1.21 watts allowable with the natural convection air cooling.

... is a reference to previous page

S N 0102-LE-014-6601

SECURITY CLASSIFICATION OF THIS PAGE (When Data Entered)

Approved for public release; distribution is unlimited

**Experiments on Liquid Immersion Natural Convection
Cooling Of Leadless Chip Carriers
Mounted on Ceramic Substrate**

by

Rufino A. Paje
Lieutenant, United States Navy
B.S., Far Eastern University, 1977

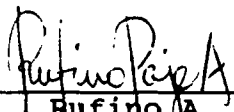
Submitted in partial fulfillment of the
requirements for the degree of

MASTER OF SCIENCE IN MECHANICAL ENGINEERING

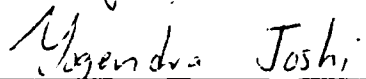
from the


NAVAL POSTGRADUATE SCHOOL
September 1989

Author:


Rufino A. Paje

Approved by:


Yogendra Joshi, Thesis Advisor


Anthony J. Healey, Chairman
Department of Mechanical Engineering

iii



Accession For	
NTIS GRA&I	<input checked="checked" type="checkbox"/>
DTIC TAB	<input type="checkbox"/>
Unannounced	<input type="checkbox"/>
Justification	
By	
Distribution/	
Availability Codes	
Dist	Avail and/or Special
A-1	

ABSTRACT

An experimental investigation of natural convection heat transfer from a commercially available semiconductor device package is presented. The package was centrally mounted on a ceramic substrate. The package-substrate assembly formed one surface of a dielectric-filled cubical enclosure of aspect ratio one. The top surface of the enclosure was maintained at prescribed temperature. Surface temperature measurements were made at various locations on the substrate, the package lid, as well as the chip center. These measurements are reported for three dielectric fluids and three enclosure top surface temperatures, both with the substrate oriented horizontally as well as vertically. Heat transfer results are also expressed in non-dimensional form. The results indicate that the maximum input power without exceeding a chip junction temperature of 80°C is 2.58 watts with FC-75 as the cooling fluid and the upper boundary maintained at 15°C . This is significantly larger than the maximum of 1.21 watts allowable with the natural convection air cooling.

TABLE OF CONTENTS

I.	INTRODUCTION.....	1
	A. MANDATES OF ADVANCING TECHNOLOGY.....	1
	B. IMMERSION COOLING: ANALYTICAL AND EXPERIMENTAL STUDIES.....	2
	C. OBJECTIVES.....	6
II.	EXPERIMENTAL SETUP.....	7
	A. COMPONENTS.....	8
	1. Heat Source Assembly.....	8
	2. The Enclosure.....	9
	3. Thermoelectric Cooling Unit.....	10
	4. Heat Exchanger.....	11
	5. Refrigerated Recirculating Bath.....	11
	6. Data Acquisition System.....	11
	7. Power Supplies.....	11
III.	EXPERIMENTAL PROCEDURES.....	13
IV.	RESULTS AND DISCUSSIONS.....	17
	A. COOLING MEDIUM: AIR,..... CHIP ORIENTATION: HORIZONTAL.	18
	B. COOLING MEDIUM: AIR,..... CHIP ORIENTATION: VERTICAL.	19
	C. COOLING MEDIUM: DIELECTRIC LIQUID..... (FLUORINERT), CHIP ORIENTATION: HORIZONTAL.	19
	D. COOLING MEDIUM: DIELECTRIC LIQUID..... (FLUORINERT), CHIP ORIENTATION: VERTICAL.	20
	E. OTHER RESULTS AND FURTHER EXPLANATIONS.....	21

V. RECOMMENDATIONS.....	23
A. APPARATUS.....	23
B. DATA ACQUISITION SYSTEM.....	23
C. LIQUID FILL-UP/BUBBLE ESCAPE PORT ASSEMBLY.....	24
APPENDIX A: SAMPLE CALCULATIONS.....	25
APPENDIX B: UNCERTAINTY ANALYSIS.....	32
APPENDIX C: TABLES.....	36
APPENDIX D: FIGURES.....	41
LIST OF REFERENCES.....	71
INITIAL DISTRIBUTION LIST.....	72

LIST OF TABLES

	Page
TABLE 1 TEMPERATURE LEVEL COMPARISON.....	37
TABLE 2 TEMPERATURE LEVEL COMPARISON.....	38
TABLE 3 TEMPERATURE LEVEL COMPARISON.....	39
TABLE 4 TEMPERATURE LEVEL COMPARISON.....	40

LIST OF FIGURES

	Page
Figure 1 Heater Assembly.....	42
Figure 2 Immersion Chamber Assembly.....	43
Figure 3 Experimental Set-up.....	45
Figure 4 Heater/Temperature Sensing Assembly.....	46
Figure 5 Thermocouple Locations.....	47
Figure 6 Liquid Immersion Enclosure.....	48
Figure 7 Bottom Plate/Heater Assembly Interface.....	49
Figure 8 Immersion Enclosure Ports.....	50
Figure 9 Heat Exchanger Assembly.....	51
Figure 10 Reference/Sensing Thermocouple Connection.....	52
Figure 11 Chip Orientations.....	53
Figure 12 Vertical Chip Orientation..... (Upper TLC Color Change)	54
Figure 13 Vertical Chip Orientation..... (Lower TLC Color Change)	55
Figure 14 Heater Assembly Thermal Response in Air..... (Horizontal Configuration)	56
Figure 15 Heater Assembly Thermal Response in Air..... (Vertical Configuration)	57
Figure 16 Heater Assembly Dimensional Thermal Response... in FC-75 (Horizontal Configuration)	58
Figure 17 Heater Assembly Dimensional Thermal Response... in FC-43 (Horizontal Configuration)	59

Figure 18	Heater Assembly Dimensional Thermal Response...60 in FC-71 (Horizontal Configuration)
Figure 19	TLC Color Display in Vertical Configuration....61
Figure 20	Heater Assembly Dimensional Thermal Response...62 in FC-75 (Vertical Configuration)
Figure 21	Heater Assembly Dimensional Thermal Response...63 in FC-43 (Vertical Configuration)
Figure 22	Heater Assembly Dimensional Thermal Response...64 in FC-71 (Vertical Configuration)
Figure 23	Heater Assembly Non-Dimensional Thermal.....65 Response in FC-75, FC-43 and FC-71 (Horizontal Configuration)
Figure 24	Heater Assembly Non-Dimensional Thermal.....66 Response in FC-75, FC-43 and FC-71 (Vertical Configuration)
Figure 25	Texas Instrument 1158 K-Factor Bar.....67
Figure 26	Film Temperature Determination.....68
Figure 27	Lid Surface Area Determination.....69
Figure 28	Package Volume Determination.....70

TABLE OF SYMBOLS AND ABBREVIATIONS

SYMBOL	DESCRIPTION	UNIT
A_{surf}	Package lid surface area	m^2
C_p	Dielectric liquid specific heat	$J/kg^\circ C$
emf	Thermocouple voltage	Volt
DAS	Data Acquisition System	Dimensionless
E_{pr}	Voltage across precision resistor	Volts
g	Gravitational Acceleration	m/s^2
H_l	Package lid height	m
H_p	Package height	m
IB	Reference ice bath thermometer scale resolution	$^\circ C$
I_R	Current through heater resistor network	Ampere
K_f	Dielectric liquid thermal conductivity	$W/m^\circ C$
L_l	Package lid length/width	m
L_p	Package length/width	m
Nu	Nusselt number	Dimensionless
Pr	Prandtl number	Dimensionless
Q_{in}	Power input to heater assembly	Watts
Ra	Rayleigh number	Dimensionless
R_{pr}	Resistance of precision resistor	Ohms
T_a	Package lid temperature based on initial TLC calibration	$^\circ C$

T_b	Package lid temperature based on final TLC calibration	$^{\circ}\text{C}$
T_c	Isothermal boundary temperature	$^{\circ}\text{C}$
TCU	Thermoelectric Cooling Unit	Dimensionless
T_{film}	Average dielectric liquid temperature	$^{\circ}\text{C}$
TLC	Thermochromic Liquid Crystal	Dimensionless
T_{lid}	Average package lid temperature	$^{\circ}\text{C}$
TSE	Temperature Sensitive Element	Dimensionless
V_{DAS}	DAS temperature readout resolution	$^{\circ}\text{C}$
V_p	Package volume	m^3
V_R	Voltage across heater resistor network	Volts
α	Dielectric liquid thermal diffusivity	m^2/s
β	Dielectric liquid thermal expansion coefficient	$1/^{\circ}\text{C}$
δ	Uncertainty of variable	Various
ν	Dielectric liquid kinematic viscosity	m^2/s
ρ	Dielectric liquid density	Kg/m^3
TC5	Isothermal Boundary Temperature (5°)	$^{\circ}\text{C}$
TC10	Isothermal Boundary Temperature (10°)	$^{\circ}\text{C}$
TC15	Isothermal Boundary Temperature (15°)	$^{\circ}\text{C}$
JUNC5	Package Junction Temperature ($T_c=5^{\circ}$)	$^{\circ}\text{C}$

JUNC10	Package Junction Temperature ($T_C=10^\circ$)	$^\circ\text{C}$
JUNC15	Package Junction Temperature ($T_C=15^\circ$)	$^\circ\text{C}$
T55	Thermocouple No. 5 Temperature ($T_C=5^\circ$)	$^\circ\text{C}$
T510	Thermocouple No. 5 Temperature ($T_C=10^\circ$)	$^\circ\text{C}$
T515	Thermocouple No. 5 Temperature ($T_C=15^\circ$)	$^\circ\text{C}$
T75	Thermocouple No. 7 Temperature ($T_C=5^\circ$)	$^\circ\text{C}$
T710	Thermocouple No. 7 Temperature ($T_C=10^\circ$)	$^\circ\text{C}$
T715	Thermocouple No. 7 Temperature ($T_C=15^\circ$)	$^\circ\text{C}$
T85	Thermocouple No. 8 Temperature ($T_C=5^\circ$)	$^\circ\text{C}$
T810	Thermocouple No. 8 Temperature ($T_C=10^\circ$)	$^\circ\text{C}$
T815	Thermocouple No. 8 Temperature ($T_C=15^\circ$)	$^\circ\text{C}$
TAMB	Ambient Temperature	$^\circ\text{C}$
TLID5	Lid Temperature ($T_C=5^\circ$)	$^\circ\text{C}$
TLID10	Lid Temperature ($T_C=10^\circ$)	$^\circ\text{C}$
TLID15	Lid Temperature ($T_C=15^\circ$)	$^\circ\text{C}$

I. INTRODUCTION

A. MANDATES OF ADVANCING TECHNOLOGY

From the inception of the first electronic digital computers to the advent of modern day supercomputers and high density power supplies of a wide array of physical dimensions and speed, it is a well accepted conclusion that long term reliability of electronic equipment is directly dependent on the thermal management scheme employed during its design. Various methods of reducing the maximum temperature, temperature gradients and fluctuations in electronic devices have been considered. These are summarized in references 1 to 7.

To gain an insight into the heat transfer problems associated with the thermal management of electronic components, let us consider some existing trends and future projections. While current developments are routinely based on chip heat fluxes of $2-3 \text{ W/cm}^2$ and peak values of 20 W/cm^2 , current research and development goals target values in excess of 100 W/cm^2 while maintaining chip surface temperatures in the range of $100-125^\circ\text{C}$. For every 2°C temperature rise in device junction temperature, reliability typically decreases by 10 percent. On the other hand, for every 20°C decrease in chip temperature, the chip failure rates decrease in half.

In response to this challenge, engineers and designers have begun to direct their attention toward the development and application of advanced thermal analysis and control techniques.

B. IMMERSION COOLING: ANALYTICAL AND EXPERIMENTAL STUDIES

To the thermal designer of microelectronic circuitry, of prime concern is the development of an efficient path for heat transfer from the heat generating device to an external cooling agent. The heat flow is typically complex and conduction, convection and radiation are often significant. Heat transfer by conduction through different materials and interfaces separating the devices from the package surface constitutes the internal conduction heat transfer processes. Some of the generated power may be radiated from the chip to the outer package surfaces. The energy is transferred from the outer walls of the package to the ambient environment often by convection. The use of liquid cooling has recently begun to be investigated in order to reduce the convective resistance.

In liquid immersion cooling, a direct physical contact is established between the cooling agent and the electronics. In order to maintain electrical isolation of the circuitry, the cooling fluid must have a high dielectric strength. Such coolants typically possess low boiling points. Their use could involve pool or forced convection

boiling, as well as single phase convection (natural, forced or mixed). The attainment of high heat transfer rates with added attractive features such as low noise and high reliability makes natural convection an attractive cooling technique.

Baker [Ref. 1] determined that free convection cooling by liquid was more than three times as effective as free convection cooling by air and for forced convection, the result was tenfold. Furthermore, [Ref. 2] it was shown that convective heat transfer coefficient would increase significantly as the size of the heat source was decreased. For a size decrease from 2.00 to 0.01 centimeter, it was determined that the convective heat transfer coefficient increased by a factor of 15.

Park and Bergles [Ref. 3] conducted experimental studies using direct-current powered thin foil heaters simulating microelectronic circuits arranged in two configurations: flush mounted and protruding from a vertical substrate. Heat transfer coefficients were obtained with varying heater heights and width in both water and R-113. The effect of height on heat transfer for single flush heaters agreed qualitatively with the conventional boundary layer theory while the widest heaters had coefficients higher than predicted due to leading edge effects. They also documented an increase in heat transfer coefficient with decreasing

width which they attributed to three-dimensional boundary layer effects. In addition, data obtained for inline and staggered arrays indicated a lower coefficient for upper heaters compared to the lower ones, with the difference diminishing as the vertical or horizontal spacing increased. Also, for the protruding heaters, the heat transfer coefficient was about 15 percent higher and the upper heaters had higher coefficients than the lower heaters.

Kelleher and Knock [Ref. 4] examined natural convection from a small heater protruding from a vertical surface of a rectangular enclosure filled with water. The enclosure vertical walls were insulated except for the heated protrusions, while the horizontal surfaces were maintained at uniform temperatures. From measured heater temperatures appropriate Nusselt and Rayleigh numbers were obtained. Results indicated that for a given Rayleigh number, the Nusselt number decreased as the heater was raised in the enclosure. Flow visualizations were also conducted, showing two flow regions: a region of buoyancy driven flow in the upper part of the enclosure and a region of flow driven by the shear interaction with the buoyancy driven region. Also indicated was the presence of small secondary cells at the upper corners of the enclosure.

A follow-on simulation of [Ref. 4] by finite differences [Ref. 5] was conducted. Comparisons of the Nusselt numbers showed good agreement for all three heater element locations in the higher Rayleigh number range, while predicted values were consistently higher in the lower Rayleigh number range.

Yang et al. [Ref. 6] carried out a three-dimensional numerical study of natural convection from nine equally spaced protrusions mounted on a vertical wall and immersed in a rectangular enclosure filled with dielectric liquid. Uniform heat fluxes were imposed on all fluid exposed element surface, while maintaining the two horizontal enclosure surfaces as uniform temperature heat sinks. It was found that temperature responses were oscillatory in nature, ranging from simple to complex. Maximum chip temperature occurred at the top rows of chips for large gap sizes. Additional numerical computations examining the effects of enclosure width were presented in a later study.

Joshi et al. [Ref. 7] conducted an experimental investigation on the natural convection cooling of a 3 by 3 array of heated protrusions in a rectangular enclosure filled with dielectric fluid FLOURINERT FC-75. It was determined that at low power levels (0.10 watts), the enclosure surface thermal conditions dictated the flow structure. An upward flow developed adjacent to each column of components with increasing power levels (0.70-3.00 watts).

It was also determined that the flow away from the elements became effectively three-dimensional and time dependent as thermal inputs were increased. Heat transfer correlations were obtained using the component surface temperatures over the range of power levels examined.

C. OBJECTIVES

This present investigation was conducted with the following goals:

1. To design and implement a natural convection liquid immersion cooling scheme for a commercial 20-pin leadless chip package.
2. To obtain and compare steady-state natural convection heat transfer characteristics of the dielectric liquid cooled arrangement with air cooling, both in horizontal and vertical heat source orientations.
3. To study the heat transfer response for a range of input component power levels, enclosure top surface boundary conditions and three dielectric liquids.

II. EXPERIMENTAL SETUP

The heat source in the entire experimentation was a leadless chip carrier mounted on a ceramic substrate [Fig. 1]. The package substrate assembly forms one surface of a dielectric liquid filled cube of inner side 4.60 centimeters. A 1.35 centimeter thick Aluminum surface with an attached thermoelectric cooling element forms a second surface of the enclosure. All other surfaces are made of lexan [Fig. 2].

An external water-cooled heat exchanger acts as the heat sink for the thermoelectric cooling unit. The cooling is provided by a Refrigerated Recirculating Bath.

Power requirements are supplied by three individually operated power supplies. The voltage outputs are monitored using the Data Acquisition System.

All external coolant flow paths and the liquid immersion chamber (enclosure) were insulated with neoprene rubber.

Information collection is accomplished with the aid of Data Acquisition System via appropriate sensing devices. The various components forming the experimental arrangement are next described [Fig. 3].

A. COMPONENTS

1. Heat Source Assembly

The heat source assembly is a Texas instrument 1158 New K-Factor Bar, 20-pin coupon leadless chip carrier centrally mounted on a ceramic substrate. The package and the substrate are squares of dimensions 1.524 millimeter and 5.08 centimeters with thicknesses of 0.381 millimeter and 0.7112 millimeter respectively. The chip consists of a transistor (Temperature Sensitive Element) for measuring junction temperature and equally distributed resistors for uniform power dissipation [Fig. 4]. The package and the upper surface of the substrate are coated with sprayable black paint (Halcrest, Glenview, Il, Type BB-M1) to provide a dark background to visualize the color patterns produced by the temperature sensitive Thermochromic Liquid Crystal (TLC). For additional thermal response measurement, nine Copper Constantan thermocouples of 0.127 millimeter diameter were bonded to the backside of the substrate starting from its center and forming 1.27 centimeters squares [Fig. 5]. Bonding was accomplished using Omega Bond 101, a high thermal conductivity adhesive.

2. The Enclosure

The liquid immersion chamber was a cube with an interior dimension of 4.60 centimeters. The bottom and side walls were constructed of 1.19 centimeter thick plexiglass while the top was of 1.35 centimeter thick Aluminum plate [Fig. 6].

The bottom plate was grooved to accommodate heater assembly thermocouple bonding protrusions. This ensured even plate-to-plate contact between interior of bottom plate and back of heater assembly. Holes of 0.7112 millimeter diameter were drilled through the bottom enclosure plate to permit thermocouple wires exit from the cube [Fig. 7].

The interior of the top plate was coated in a manner similar to the heater assembly for ThermoChromic Liquid Crystal (TLC) calibration.

Approximately 1.27 centimeters diagonally from one of the corners, a 2.95 millimeter hole was drilled at an angle of about 70° to serve as liquid fill-up port and air bubble escape path. Two additional holes of 2.95 millimeter diameter were drilled at identical angles of about 40° terminating at 4.76 millimeters from the bottom of the plate and 2.54 centimeters apart [Fig. 8]. These holes acted as thermocouple placement ports for monitoring the upper boundary temperature. Once again, OMEGA 101 bonding compound was used to fill the gaps between the thermocouple wires and holes.

The cube assembly was sealed with the use of both rubber O-Rings and General Electric RTV adhesive/sealant.

Air bubbles which developed inside the enclosure during the conduct of experiment were ejected by a series of short strokes of a syringe attached to one end of a plastic tubing whose other end was attached to the fill-up port/bubble escape path of the liquid immersion cube. The strokes created a disruption on the bubbles and in conjunction with the proper liquid immersion tilt angle, they resulted in bubble movement towards the escape port and eventually up the syringe. The syringe and the plastic tubing were filled with dielectric liquid at all times.

3. Thermoelectric Cooling Unit

The cooler is a sub-miniature thermoelectric heat pump in modular form. It utilized ceramic plates for high electrical insulation and thermal conductivity. It was a MELCHOR FRIGICHIP model CP 1.4-127-10L.

Thermoelectric couples were made from two elements of semiconductor, primarily by Bismuth Telluride, heavily doped to create either an excess N-type or P-type of electrons. Heat absorbed at the cold junction was pumped to the hot junction at a rate proportional to carrier current passing through the circuit and the number of couples. The hot junction eventually expelled the heat.

4. Heat Exchanger

The heat exchanger was a locally manufactured double-path system constructed of Aluminum. Inlet and outlet ports were provided for the attachment of Brass fittings for plastic tubing connections to convey cooling water from and to the Refrigerated Circulating Bath [Fig. 9].

5. Refrigerated Recirculating Bath

This component provided external cooling water for the heat exchanger. It was a NESLAB ENDOCAL model RTE-5B. The base was shock mounted with rubber to minimize the transmission of vibration to the liquid immersion assembly thus minimizing disruption of natural circulation flow patterns.

6. Data Acquisition System

The data acquisition system was a HP-3852A model. Pertinent connections to sensors were made via a model HP-44705A multiplexer and model HP-44701A voltmeter.

A separate computer program using a fourth order polynomial was written to convert measured voltages into temperatures.

7. Power Supplies

Power supply No. 1 was a model HP-6289A capable of supplying 0-1.80 amperes and 0-50 volts. It provided the specific power levels to the heat dissipating component of

the heater assembly. Another identical power supply provided the required current to activate the Temperature Sensitive Element (TSE) component of the heater assembly. The third power supply was a model HP-6214B capable of supplying 0-1.20 amperes and 0-12 volts. It was used to power the Thermoelectric Cooling Unit.

III. EXPERIMENTAL PROCEDURE

Initial experiments examined the natural convection response of the electronic package with the application of specified power levels in air. With the chip-substrate combination attached to the bottom plate of the immersion cube [II.A.2], the plate was placed inside a cardboard box of length 29.2 centimeters, width 24.1 centimeters and height 29.2 centimeters without a lid. This procedure was designed to achieve a quiescent ambient condition by preventing the effects of circulating air currents from affecting the thermal response of the package. At the conclusion of this portion of the experiment, the side walls and the top of the enclosure were attached and the enclosure filled with dielectric liquid. It was then mounted on an ordinary laboratory stand that was supported by brackets to eliminate lateral motion. Additional minute quantity of dielectric liquid required to completely fill up the cube was introduced via the fill-up/air bubble escape port [II.A.2.]. Proper horizontal or vertical chip orientation was maintained with a carpenter's level.

The Refrigerated Recirculating Bath temperature control knob was permanently set at 15°C with adhesive tape to prevent inadvertent changes in temperature setting.

The Thermoelectric Cooling Unit positive terminal was connected to the positive terminal of its power supply and the negative terminals were connected together. This was critical in achieving its function as heat sink and maintaining an isothermal wall boundary condition.

Thermocouple reference temperature of 0°C was obtained with the use of crushed ice-water mixture. A mercury thermometer inserted into the ice bath ensured that the temperature was at $0 \pm 0.05^{\circ}\text{C}$. Each reference thermocouple was connected such that its constantan leads was connected to the constantan lead of the measurement thermocouple. The copper leads were directly connected to the Data Acquisition System multiplexer. Each measurement thermocouple was individually referenced to the ice bath [Fig. 10].

The following steps were followed during a typical experiment:

1. The heater assembly was analyzed in two configurations. The horizontal configuration was such that the heater assembly was at the bottom of the immersion cube and the Aluminum wall at the top. A 90° rotation in the vertical plane [Fig. 11] resulted in the vertical configuration.

For the study, five power input levels were applied to the heat dissipating component. Thermochromic Liquid Crystal (TLC) color changes were observed using a regular Halogen bulb flashlight. Current supply to the Temperature Sensitive Element (TSE) was maintained at -1.0 milliamperes.

2. TLC Color/Temperature Calibration:
The liquid crystal changed colors in response to temperature variation brought about by the application of various specified power levels. These color

changes resulted from the reorientation (rotation) of the crystal's lattice such that different wavelengths of light are reflected depending on the temperature. Calibration was accomplished at room temperature with normal room lighting conditions, using the following steps:

- (a) The lowest possible power level was applied until the clear TLC color shifted to the first discernible green. A settling time of approximately 1.0 hour was allotted.
 - (b) Power was then incrementally reduced until the TLC color attained in step (a) just disappeared.
 - (c) Power was incrementally raised until the color in step (a) was reached.
 - (d) The temperature at the appearance of color was measured by two thermocouples attached to the Aluminum plate.
 - (e) Steps (a)-(c) were repeated for the full range of color display, while maintaining the TSE current supply at -1.0 milliamp. TLC shifted to its clear coating appearance at higher temperatures. The sequence of events was recorded by a high speed video camera.
3. (a) Prior to each experiment, the Data Acquisition System was activated and the power supply to the TSE was switched on and properly adjusted to deliver a -1.0 milliamper current. After a settling period of approximately 30 minutes, a set of measurements of the TSE junction temperature and the chip ceramic substrated mounted thermocouples were taken using the Data Acquisition System. This step was designed to verify the agreement between the TSE and the thermocouples at room temperature without the application of power to the chip resistor assembly.
- (b) At this time, the Refrigerated Recirculating Bath and the power supplies for the Thermoelectric Cooling Unit and the resistor network of the chip assembly were energized. The Thermoelectric Cooling Unit power supply was so adjusted that a nearly isothermal

enclosure top wall condition was indicated by the pair of monitoring thermocouples [II.A.2]. Measurements were made for three settings of 5, 10 and 15°C. The resistor network power supply was adjusted until the TLC coating of the chip lid first turned green, signifying power level 1. Incremental adjustments of the TCU and resistor network power supplies were made until the desired upper boundary temperature and green color on the package lid were attained. Due to TSE sensitivity to temperature variation, it was mandatory to verify that its current supply was indeed -1.0 milliampere. After a settling period of approximately 2 hours to enable the attainment of a steady-state thermal response, measurements of temperature responses on the chip and substrate were initiated. These measurements were taken every 10 minutes until successive measured temperatures remained unchanged within $\pm 0.05^\circ\text{C}$ at each location.

- (c) With the same upper boundary condition, resistor power was incrementally increased until the green color shifted to turquoise (power level 2). Following another series of incremental power supply adjustments, desired settings of the upper boundary temperature and the turquoise color were obtained. The same process continued until the maximum TSE junction temperature of approximately 80°C with its corresponding color change was obtained, reflecting power level 5. Power levels 3 and 4 were incremented between 2 and 5.
- (d) The immersion cube was then rotated 90° along the vertical plane for the vertical orientation portion of the experiment. Identical procedural steps as for the horizontal orientation were followed with the exception that color changes were observed as depicted in figure 12. Two additional power levels and their corresponding color change were observed as depicted in figure 13.

IV. RESULTS AND DISCUSSIONS

A typical experiment resulted in the following heat flow path. As specified power was applied to the heat dissipating component, part of the generated power is conducted to the outer package as well as to the substrate. There is also a direct radiation contribution from the chip to the outer package walls. From the package lid and the substrate the energy is convected by the liquid primarily to the thermoelectric cooled Aluminum wall. Some of the energy is also conducted across the lexan walls of the enclosure. The heat transferred to the Aluminum wall is once again transmitted by conduction across the thermoelectric cooling unit and eventually to the cooling water of an external heat exchanger assembly.

Analysis of experimental results on the thermal response of the package and substrate is discussed in this chapter. It includes comparison of thermal responses in air and dielectric liquids as cooling mediums. The junction temperature sensor, thermocouple readouts and the Thermochromic Liquid Crystal (TLC) color changes provide the pertinent information presented.

Results are presented both in dimensional and non-dimensional forms. Dimensional measurements included the applied power and the resulting temperature levels. Non-

dimensional data are presented as Nusselt and Rayleigh numbers, which are defined as follows:

a) Nusselt Number, Nu

$$Nu = \frac{(Q_{in})(A_{surf})}{(V_p)(K_f)(T_{lid} - T_c)} \quad (1)$$

b) Rayleigh Number, Ra

$$Ra = \frac{(g)(\beta)(A_{surf})(Q_{in})}{(\nu)(\alpha)(K_f)} \quad (2)$$

In this study, Nusselt number represents the inverse of the non-dimensional component lid temperature excess, while Rayleigh number represents the non-dimensional component input power level.

A. COOLING MEDIUM: AIR, CHIP ORIENTATION: HORIZONTAL

It is discernible from figure 14 that the temperature levels at the chip and various substrate locations increase with the application of power. It was also noted that the thermal responses at the various substrate locations depend on their proximity to the heat dissipating element of the assembly. This is demonstrated by the appropriate "isothermal color rings" of the TLC coating of the assembly. These color patterns demonstrate an almost symmetric behavior about the package center.

B. COOLING MEDIUM: AIR, CHIP ORIENTATION: VERTICAL

As in figure 14 all temperatures increase with increasing powers. The resulting levels are seen in figure 15. However, the simple direct relationship between thermal response at a substrate location and the proximity to the chip is changed due to the action of buoyancy forces. A natural convection flow in which heated air rises vertically entraining fluid from the quiescent ambient region results adjacent to the package. This flow contributed to lower temperatures of monitored points above the package compared with points located below the package as denoted by table 1. The buoyant upflow adjacent to the package results in a wall plume-like flow, causing an asymmetry in the surface temperature contours.

**C. COOLING MEDIUM: DIELECTRIC LIQUID (FLOURINERT),
CHIP ORIENTATION: HORIZONTAL**

As with air, analysis of results showed that for the three dielectric fluids thermal responses were likewise directly proportional to applied power. Once again direct relationship between thermal response and proximity to heat source was exhibited. The TLC color displays were in the form of "isothermal color rings".

Figures 16, 17 and 18 demonstrate that there was minimal effect of isothermal boundary conditions used in the study on

the resulting thermal response of the assembly. By employing the temperature difference ($T_i - T_c$), data for various T_c followed the same variation.

**D. COOLING MEDIUM: DIELECTRIC LIQUID (FLOURINERT),
CHIP ORIENTATION: VERTICAL**

In the vertical orientation, immersion of the package in dielectric liquids confined by an enclosure revealed differences in transport behavior compared to the unconfined air measurements. Temperatures of monitored points on the substrate located above the packages showed temperatures higher than those located below as shown by table 2, 3 and 4. This results due to the convected energy of the buoyant upflow being transferred partially to the substrate. This is in contrast to the measurements in air where the vigorous convective motion actually results in a decrease in the substrate temperature above the package compared to locations below. In the vertical orientation, the isotherms were of an elliptical shape that is offset from the package center with the major axis oriented vertically [Fig. 19]. The observance of this phenomena was more pronounced at the lower power levels.

Just as was the case for horizontal orientation, it was determined that changing the isothermal boundary temperature had minimal impact on the temperature excess levels at various locations. This is exhibited by figure 20, 21 and 22.

E. OTHER RESULTS AND FURTHER EXPLANATIONS:

1. Comparison between temperatures measured by thermocouples no. 4 located above the package and no. 6 located below the package are listed in tables 1, 2, 3 and 4. Analysis of this observed behavior is attributed to the following:

Air has a viscosity substantially lower than any of the dielectric liquids used in this study. As such, for a given input power level the greater velocity attained in air cooling due to buoyancy forces contribute to a cooling effect. The lower velocity in the dielectric liquid cooling actually causes a portion of the transported heat to be transferred into the substrate, resulting in a heating effect.

2. It was determined that the liquid possessing the lowest Prandtl number was the most efficient coolant. In this study it turns out to be FC-75. For a junction temperature of 80°C in the horizontal orientation, natural convection air cooling allowed a maximum power input of 1.21 watts at ambient temperature of 20°C. The three dielectric fluids FC-75, FC-43 and FC-71 allowed 1.87, 1.78 and 1.53 watts respectively at an isothermal boundary temperature of 15°C. These data confirm the slight advantage of liquid immersion cooling over natural convection air cooling for this package. However, it is found based on figures 17-22 that the bulk of the thermal resistance is encountered between the junction and the lid. This resistance is largely unaffected by the improved convection environment. Thus in

order to make the greatest use of the improved convective heat transfer, a package design with substantially smaller internal thermal resistance would be needed.

3. In both cases of air cooling [Figs, 14, 15] and liquid immersion cooling [Figs. 17-24], it was determined that chip orientation did not have a profound effect on the junction temperatures. It was noted however, that the two dielectric liquids with the lowest Prandtl numbers resulted in somewhat lower junction temperatures in the horizontal orientation. Greater lid temperature uniformity and more efficient heat removal by the heat exchanger further makes the horizontal configuration more advantageous.

V. RECOMMENDATIONS

A. APPARATUS

A crucial aspect of the experiment is a proper management of the heater assembly. Care should be observed during the application of a thin coat background black paint followed by the TLC. Another important step is the proper bonding of the thermocouples to the back side of the ceramic substrate.

The present study has investigated the 20-pin type package. It is recommended that larger size packages be examined using the same experimental arrangement.

When trying to determine the color display of the TLC, it must be borne in mind that the thermal radiation from a regular Halogen flashlight is enough to cause thermal disruption. It is most strongly recommended that such light flashing activities be executed expeditiously and time be allotted for the reattainment of thermal steady state prior to obtaining additional data.

B. DATA ACQUISITION SYSTEM

A computer and a plotter should be interfaced with the system so the results could be handily analyzed. Data acquisition programs should be written to include data gathering, storage and dissemination.

C. LIQUID FILL-UP/BUBBLE ESCAPE PORT ASSEMBLY

It is recommended that the hose joining the syringe and the immersion enclosure fill-up/bubble escape port be shortened to about a third of its existing length to facilitate accomplishment of intended purpose.

APPENDIX A

SAMPLE CALCULATIONS

NOTE: ALL PARAMETERS USED IN CALCULATIONS ARE DEFINED IN
THE TABLE OF SYMBOLS AND ABBREVIATIONS.

A. DETERMINATION OF INPUT POWER, Q_{in} (watts)

From Figure 25,

$$\begin{aligned} Q_{in} &= (V_R)(I_R) \\ &= (V_R)(E_{pr}) \end{aligned}$$

CALCULATION: For FLOURINERT (FC-75), power dissipation at
power level 1, $T_c=15^\circ\text{C}$, horizontal configuration.

$$\begin{aligned} Q_{in} &= (19.01)(14.78/140) \\ &= 2.01 \text{ watts} \end{aligned}$$

B. THERMOCOUPLE CONVERSION FROM VOLTAGE (emf) TO TEMPERATURE ($^\circ\text{C}$).

HP 3852A Data Acquisition System (Channels 1-9 and 11-12)
records voltage readings in millivolts (mv) and convert them
to temperatures ($^\circ\text{C}$). The coefficients are designed for OMEGA
Copper-Constantan thermocouples.

$$\begin{aligned} T(^{\circ}\text{C}) &= 0.0006797 + 25825.1328 * \text{emf} - 607789.2467 * \text{emf}^{**2} \\ &\quad - 21952034.3364 * \text{emf}^{**3} + 8370810996.1874 * \text{emf}^{**4} \end{aligned}$$

CALCULATION: For FLOURINERT (FC-75), power level 1, $T_\gamma=5^\circ\text{C}$,
horizontal configuration, thermocouple No. 1.

$$T_1 = 0.0006797 + 25825.1328 * 0.00063213 - 607789.2467 * 0.00063213^{**2} \\ - 21952034.3364 * 0.00063213^{**3} + 8370810996.1874 * 0.00063213^{**4} \\ = 16.08^{\circ} \text{C}$$

C. CHIP LID TEMPERATURE, T_{lid}

$$T_{lid} = (T_a + T_b) / 2$$

CALCULATION: For FLOURINERT (FC-75), power level 1, $T_c = 5^{\circ} \text{C}$, horizontal configuration.

$$T_{lid} = (29.4 + 28.5) / 2 \\ = 29.0^{\circ} \text{C}$$

D. FILM TEMPERATURE, T_{film}

From Figure 26,

$$T_{film} = \frac{(T_c + T_{lid})}{2}$$

CALCULATION: For FLOURINERT (FC-75), power level 1, $T_c = 5^{\circ} \text{C}$ horizontal configuration.

$$T_{film} = (5 + 29) / 2 \\ = 17.0^{\circ} \text{C}$$

E. FLUID PROPERTY DETERMINATION

We note that T_{film} is in $^{\circ} \text{C}$ in all fluid properties correlations listed below.

1. Thermal Conductivity, $K_f (W/m^{\circ} \text{C})$

From Figure 5 of the 3M corporation FLOURINERT product manual, the thermal conductivity coefficient curves have been determined to be:

(a) FC-75

$$K_f = 0.065 - 7.89474E-05 * T_{\text{film}}$$

(b) FC-43

$$K_f = 0.06660 - 9.864E-06 * T_{\text{film}}$$

(c) FC-71

$$K_f = 0.071$$

CALCULATION: For FLOURINERT (FC-75), power level 1, $T_c = 5^\circ\text{C}$
horizontal configuration.

$$K_f = 0.065 - 7.89474E-05 * 17.0$$

$$= 0.0637 \text{ W/m}^\circ\text{C}$$

2. Density, ρ (Kg/m₃)

Using the expression on table 4B and constants
presented in table 4C of the product manual:

(a) FC-75

$$\rho = (1.825 - 0.00246 * T_{\text{film}}) * 1000$$

(b) FC-43

$$\rho = (1.913 - 0.000218 * T_{\text{film}}) * 1000$$

(c) FC-71

$$\rho = (2.002 - 0.00224 * T_{\text{film}}) * 1000$$

CALCULATION: For FLOURINERT (FC-75), power level 1, $T_c = 5^\circ\text{C}$
horizontal configuration.

$$\rho = (1.825 - 0.00246 * 17.0) * 1000$$

$$= 1783.18 \text{ Kg/m}^3$$

3. Kinematic Viscosity, ν (m^2/s)

From figure 3 and determining a 4th order polynomial curve fit gives:

(a) FC-75

$$\nu = [1.4074 - 2.96\text{E-}02 * T_{\text{film}} + 3.8018\text{E-}04 * T_{\text{film}}^{**2} - 2.7308\text{E-}06 * T_{\text{film}}^{**3} + 8.1679\text{E-}09 * T_{\text{film}}^{**4}] 1\text{E-}06$$

(b) FC-43

$$\nu = [8.8750 - 0.47007 * T_{\text{film}} + 1.387\text{E-}02 * T_{\text{film}}^{**2} - 2.1469\text{E-}04 * T_{\text{film}}^{**3} + 1.3139\text{E-}06 * T_{\text{film}}^{**4}] 1\text{E-}06$$

(c) FC-71

$$\nu = [251.62 - 13.723 * T_{\text{film}} + 0.30561 * T_{\text{film}}^{**2} - 3.1704\text{E-}03 * T_{\text{film}}^{**3} + 1.2668\text{E-}05 * T_{\text{film}}^{**4}] 1\text{E-}06$$

CALCULATION: For FLOURINERT (FC-75), power level 1, $T_c = 5^\circ\text{C}$, horizontal configuration.

$$\begin{aligned} \nu &= [1.4074 - 2.96\text{E-}02 * 17.0 + 3.8018\text{E-}04 * 17.0^{**2} \\ &\quad - 2.7308\text{E-}06 * 17.0^{**3} + 8.1679\text{E-}09 * 17.0^{**4}] 1\text{E-}06 \\ &= 1.0013\text{E-}06 \text{ m}^2/\text{s} \end{aligned}$$

4. Specific Heat, C_p ($\text{J/Kg}^\circ\text{C}$)

For all FLOURINERT electrochemicals, figure 4 of the product manual:

$$C_p = (0.241111 + 3.70374\text{E-}04 * T_{\text{film}}) * 4186$$

CALCULATION: For FLOURINERT (FC-75), power level 1, $T_c = 5^\circ\text{C}$, horizontal configuration.

$$\begin{aligned} C_p &= (0.241111 + 3.70374\text{E-}04 * 17.0) * 4186 \\ &= 1035.65 \text{ J/Kg}^\circ\text{C} \end{aligned}$$

5. Thermal Diffusivity, α (m^2/s)

From $\alpha = K_f / (\rho * C_p)$

CALCULATION: For FLOURINERT (FC-75), power level 1, $T_c = 5^\circ \text{C}$, horizontal configuration.

$$\begin{aligned}\alpha &= 0.0637 / (1783.18 * 1035.65) \\ &= 3.449\text{E-}08 \text{ m}^2/\text{s}\end{aligned}$$

6. Thermal Expansion Coefficient, β ($1/^\circ \text{C}$)

Using expression in table 4B and the constants from table 4C (3M product manual) yields:

(a) FC-75

$$\beta = 0.00246 / (1.825 - 0.00246 * T_{\text{film}})$$

(b) FC-43

$$\beta = 0.00218 / (1.913 - 0.00218 * T_{\text{film}})$$

(c) FC-71

$$\beta = 0.00224 / (2.002 - 0.00224 * T_{\text{film}})$$

CALCULATION: For FLOURINERT (FC-75), power level 1, $T_c = 5^\circ \text{C}$, horizontal configuration.

$$\begin{aligned}\beta &= 0.00246 / (1.825 - 0.00246 * 17) \\ &= 0.00138 / ^\circ \text{C}\end{aligned}$$

F. LID SURFACE AREA, A_{surf} (m^2) DETERMINATION

From figure 27,

CALCULATION:

$$\begin{aligned}
A_{\text{surf}} &= 4L_1H_1 + L_1^2 \\
&= (4 \times 0.889 \times 0.18542) + (0.889)^2 \\
&= 1.4496745 \text{ cm}^2 \\
&= 1.4496\text{E-}04 \text{ m}^2
\end{aligned}$$

G. PACKAGE VOLUME, $V_p(\text{m}^3)$ DETERMINATION

From figure 28

CALCULATION:

$$\begin{aligned}
V_p &= L_p^2 H_p \\
&= (0.1524)^2 \times (0.0381) \\
&= 8.849\text{E-}04 \text{ cm}^3 \\
&= 8.849\text{E-}10 \text{ m}^3
\end{aligned}$$

H. NON-DIMENSIONAL PARAMETER DETERMINATION

1. Nusselt Number, Nu

$$Nu = (Q_{\text{in}} \times A_{\text{surf}}) / [V_p \times K_f \times (T_{\text{lid}} - T_c)]$$

CALCULATION: For FLOURINERT (FC-75), power level 1, $T_c = 5^\circ\text{C}$, horizontal configuration.

$$\begin{aligned}
Nu &= (2.01 \times 1.4496\text{E-}04) / [8.849\text{E-}10 \times 0.0637 \times (29.0 - 5.0)] \\
&= 2.1538\text{E}05
\end{aligned}$$

2. Rayleigh Number, Ra

$$Ra = (g \times \beta \times A_{\text{surf}} \times Q_{\text{in}}) / (\nu \times K_f)$$

CALCULATION: For FLOURINERT (FC-75), power level 1, $T_c = 5^\circ\text{C}$, horizontal configuration.

$$\begin{aligned}
 Ra &= (9.81 * 0.00138 * 1.4496E-04 * 2.01) / (1.0013E-06 * 3.449E \\
 &\quad -08 * 0.0637) \\
 &= 1.793E09
 \end{aligned}$$

I. PRANDTL NUMBER, Pr DETERMINATION

From the definition of Prandtl Number,

$$Pr = \nu / \alpha$$

CALCULATION: For FLOURINERT (FC-75), power level 1, $T_c = 5^\circ\text{C}$, horizontal configuration.

$$\begin{aligned}
 Pr &= (1.0013E-06) / (3.449E-08) \\
 &= 29.03
 \end{aligned}$$

APPENDIX B

UNCERTAINTY ANALYSIS

CALCULATION: For FLOURINERT (FC-75), power level 1, $T_c=5^\circ\text{C}$
horizontal configuration.

A. NUSSELT NUMBER, Nu

Assuming no uncertainty in the values if the
thermophysical properties, eqn. (1) in Chapter 4 yields:

$$\left(\frac{\delta Nu}{Nu}\right) = \left[\left(\frac{\delta Q_{in}}{Q_{in}}\right)^2 + \left(\frac{\delta A_{surf}}{A_{surf}}\right)^2 + \left(\frac{\delta V_p}{V_p}\right)^2 + \left(\frac{\delta \Delta T}{\Delta T}\right)^2 \right]^{\frac{1}{2}}$$

where:

$$a) \left(\frac{\delta Q_{in}}{Q_{in}}\right) = \left[\left(\frac{\delta V_R}{V_R}\right)^2 + \left(\frac{\delta I_R}{I_R}\right)^2 + \left(\frac{\delta R_{pr}}{R_{pr}}\right)^2 \right]^{\frac{1}{2}}$$

where:

$$i) \left(\frac{\delta V_R}{V_R}\right) \quad \text{where:}$$

$\delta V_R = 10^{-6} \text{ volt (Manufacturer Data)}$

$V_R = 14.77842 \text{ volts (Measured Data)}$

Calculation:

$$\begin{aligned} \left(\frac{\delta V_R}{V_R}\right) &= 10^{-6}/14.77842 \\ &= 6.7666\text{E-}08 \end{aligned}$$

$$ii) \left(\frac{\delta I_R}{I_R} \right) = \left[\left(\frac{\delta V_R}{V_R} \right)^2 + \left(\frac{\delta R_{pr}}{R_{pr}} \right)^2 \right]^{\frac{1}{2}}$$

where:

$$\delta R_{pr} = 0.01 \text{ (Manufacturer Data)}$$

$$R_{pr} = 140 \text{ ohms (Measured Data)}$$

$$\begin{aligned} \text{Calculation: } \left(\frac{\delta R_{pr}}{R_{pr}} \right) &= (0.01)/(140.0) \\ &= 7.14286E-05 \end{aligned}$$

Calculation:

$$\begin{aligned} \left(\frac{\delta I_R}{I_R} \right) &= [(6.7666E-08)^2 + (7.14286E-05)^2]^{\frac{1}{2}} \\ &= 7.14286E-05 \end{aligned}$$

Calculation:

$$\begin{aligned} \left(\frac{\delta Q_{in}}{Q_{in}} \right) &= [(6.7666E-08)^2 + (7.14286E-05)^2 + (7.14286E-05)^2]^{\frac{1}{2}} \\ &= 1.01015E-04 \end{aligned}$$

$$b) \left(\frac{\delta A_{surf}}{A_{surf}} \right) = \frac{((4L_1 \delta H_1)^2 + [(4H_1 + 2L_1)(\delta L_1)]^2)^{\frac{1}{2}}}{[(4H_1 L_1) + (L_1)^2]}$$

where:

$$L_1 = 8.89E-03m \text{ (Manufacturer Data)}$$

$$H_1 = 1.8542E-03m \text{ (Manufacturer Data)}$$

$$\delta L_1 = \delta H_1 = 2.54E-05E-05m \text{ (Manufacturer Data)}$$

Calculation:

$$\left(\frac{\delta A_{\text{surf}}}{A_{\text{surf}}} \right) = \frac{((4 * 8.89E-03 * 2.54E-05)^2 + [(4 * 1.8542E-03 + 2 * 8.89E-03) (2.54E-05)]^2)^{\frac{1}{2}}}{[(4 * 1.8542E-03 * 8.89E-03) + (8.89E-03)^2]} = 7.6361E-03$$

$$c) \left(\frac{\delta V_p}{V_p} \right) = \left[\left(\frac{2 \delta L_p}{L_p} \right)^2 + \left(\frac{\delta H_p}{H_p} \right)^2 \right]^{\frac{1}{2}}$$

where:

$$L_p = 1.524E-03 \text{m (Manufacturer Data)}$$

$$H_p = 3.81E-04 \text{m (Manufacturer Data)}$$

$$\delta H_p = \delta L_p = 2.54E-05 \text{m (Manufacturer Data)}$$

Calculation:

$$\left(\frac{\delta V_p}{V_p} \right) = \left[\left(\frac{2 * 2.54E-05}{1.524E-03} \right)^2 + \left(\frac{2.54E-05}{3.81E-04} \right)^2 \right]^{\frac{1}{2}} = 7.45356E-02$$

$$d) \left(\frac{\delta \Delta T}{\Delta T} \right) = [(\delta V_{\text{DAS}})^2 + (\delta I_B)^2]^{\frac{1}{2}} + \delta \text{ curve}$$

where:

$$\delta V_{\text{DAS}} = 0.025^\circ \text{C (Manufacturer Data)}$$

$$\delta I_B = 0.05^\circ \text{C (Manufacturer Data)}$$

solving for $\delta \text{ curve}$:

From TABLE IV of OMEGA ENGINEERING, for Copper Constantan Thermocouple at 40°C, thermoelectric voltage is

1.611 mV. Using the 4th degree polynomial curve fit (item B of Appendix A), the corresponding temperature for 1.611 mV is 39.9921265°C. The δ curve value is calculated as

$$40.00 - 39.9921265 = 7.874\text{E-}03$$

Calculation:

$$\begin{aligned} \left(\frac{\delta \Delta T}{\Delta T} \right) &= [(0.025)^2 + (0.05)^2]^{\frac{1}{2}} + 7.874\text{E-}03 \\ &= 6.37757\text{E-}02 \end{aligned}$$

Calculation:

$$\begin{aligned} \left(\frac{\delta Nu}{Nu} \right) &= \\ &= [(1.01015\text{E-}04)^2 + (7.6361\text{E-}03)^2 + (7.45356\text{E-}02)^2 + (6.37757\text{E-}02)^2]^{\frac{1}{2}} \\ &= 9.83932\text{E-}02 \end{aligned}$$

B. RAYLEIGH NUMBER, Ra

$$\left(\frac{\delta Ra}{Ra} \right) = \left[\left(\frac{\delta A_{\text{surf}}}{A_{\text{surf}}} \right)^2 + \left(\frac{\delta Q_{\text{in}}}{Q_{\text{in}}} \right)^2 \right]^{\frac{1}{2}}$$

Calculation:

$$\begin{aligned} \left(\frac{\delta Ra}{Ra} \right) &= [(7.6361\text{E-}03)^2 + (1.01015\text{E-}04)^2]^{\frac{1}{2}} \\ &= 1.079955\text{E-}02 \end{aligned}$$

These calculated uncertainty values are intended to be representative examples of the overall uncertainty for this study.

APPENDIX C

TABLES

TABLE I. TEMPERATURE LEVEL COMPARISON

		COOLANT: AIR CHIP ORIENTATION: VERTICAL	
POWER LEVEL	POWER WATTS	$T_4, ^\circ\text{C}$	$T_6, ^\circ\text{C}$
1	0.36	26.7	27.3
2	0.40	27.0	27.5
3	0.63	32.8	33.4
4	0.92	35.4	36.3
5	1.25	39.7	40.9

TABLE II. TEMPERATURE LEVEL COMPARISON

POWER LEVEL	POWER WATTS	COOLANT: FC-75 CHIP ORIENTATION: VERTICAL	
		$T_c = 15^\circ\text{C}$	
		$T_4, ^\circ\text{C}$	$T_6, ^\circ\text{C}$
1	0.98	24.3	22.2
2	1.08	24.8	22.5
3	1.31	26.2	23.5
4	1.56	27.9	24.7
5	1.84	29.2	25.4

TABLE III. TEMPERATURE LEVEL COMPARISON

		COOLANT: FC-43 CHIP ORIENTATION: VERTICAL	
POWER LEVEL	POWER WATTS	$T_c = 15^\circ \text{C}$	
		$T_4, ^\circ \text{C}$	$T_6, ^\circ \text{C}$
1	0.81	24.6	22.8
2	0.88	24.8	22.9
3	1.13	27.1	24.6
4	1.42	29.1	27.7
5	1.74	31.4	27.7

TABLE IV. TEMPERATURE LEVEL COMPARISON

		COOLANT: FC-71 CHIP ORIENTATION: VERTICAL	
POWER LEVEL	POWER WATTS	$T_C = 15^\circ\text{C}$	
		$T_4, ^\circ\text{C}$	$T_6, ^\circ\text{C}$
1	0.52	25.7	24.6
2	0.57	26.1	25.1
3	0.83	28.6	27.1
4	1.13	32.1	29.9
5	1.49	37.2	34.2

APPENDIX D

FIGURES

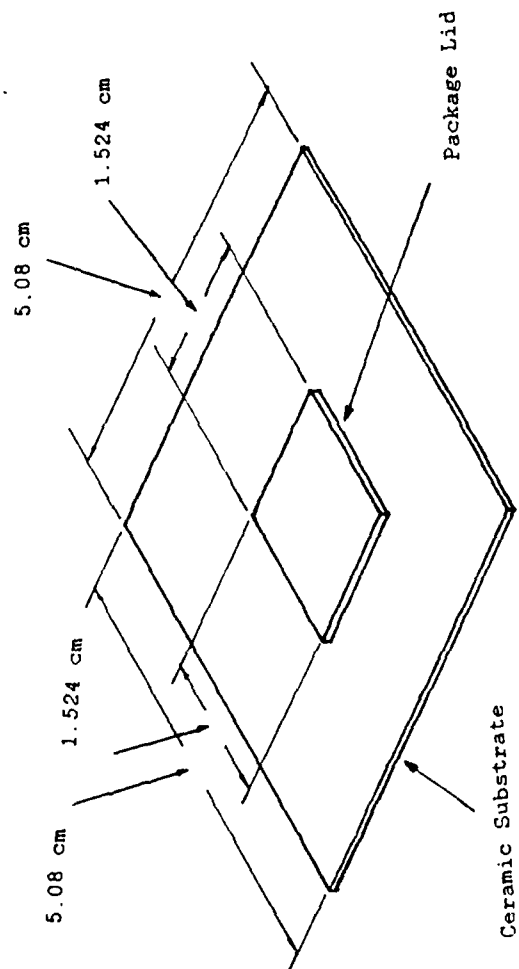


Figure 1. Heater Assembly

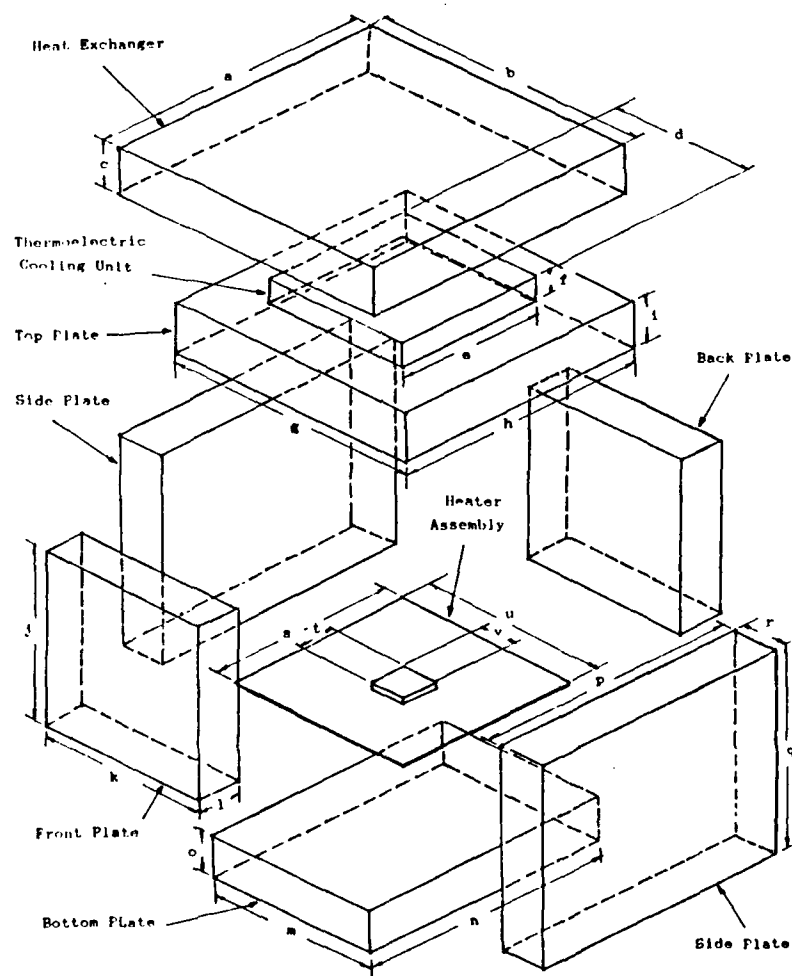


Figure 2. Immersion Chamber Assembly
(For Dimensions refer to following page)

DESIGNATION**DIMENSION**

a	7.62 cm
b	7.239 cm
c	1.27 cm
d	4.00 cm
e	4.10 cm
f	0.47 cm
g	6.985 cm
h	6.985 cm
i	1.35 cm
j	4.60 cm
k	4.60 cm
l	1.19 cm
m	4.60 cm
n	6.985 cm
o	1.19 cm
p	6.985 cm
q	5.64 cm
r	1.19 cm
s	5.08 cm
t	0.889 cm
u	5.08 cm
v	0.889 cm

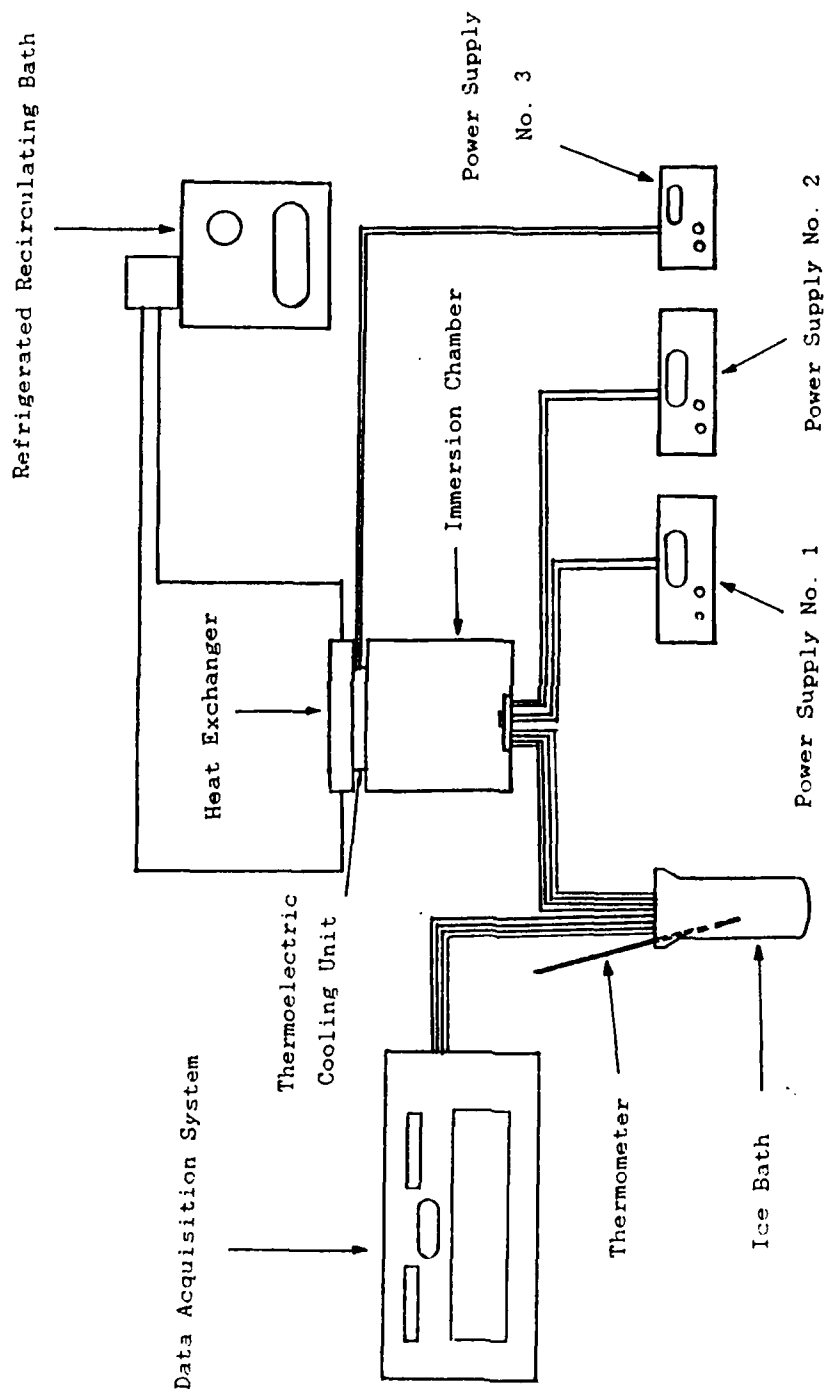


Figure 3. Experimental Set-up

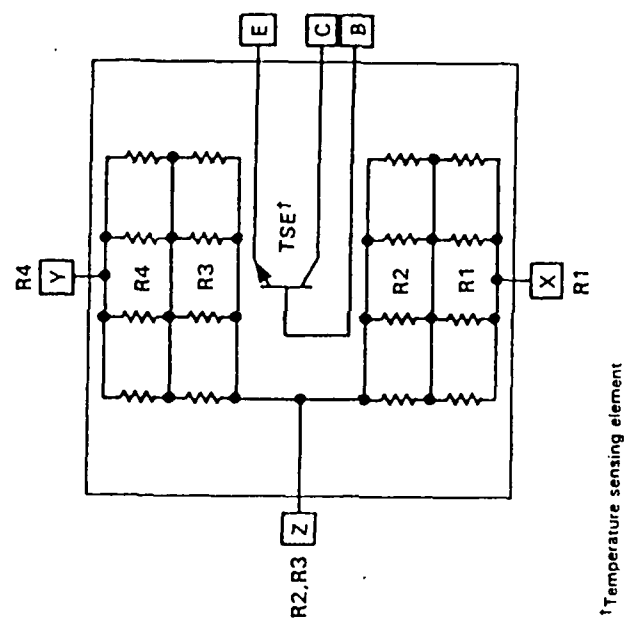


Figure 4. Heater/Temp Sensing Assembly

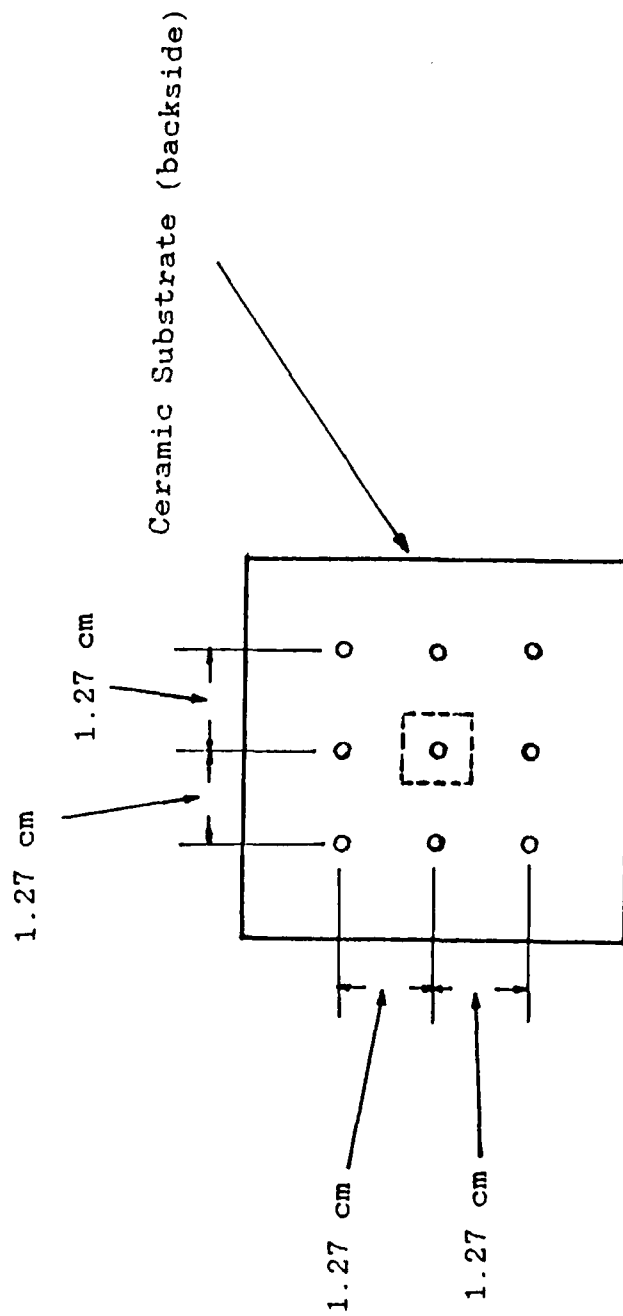


Figure 5. Thermocouple Locations

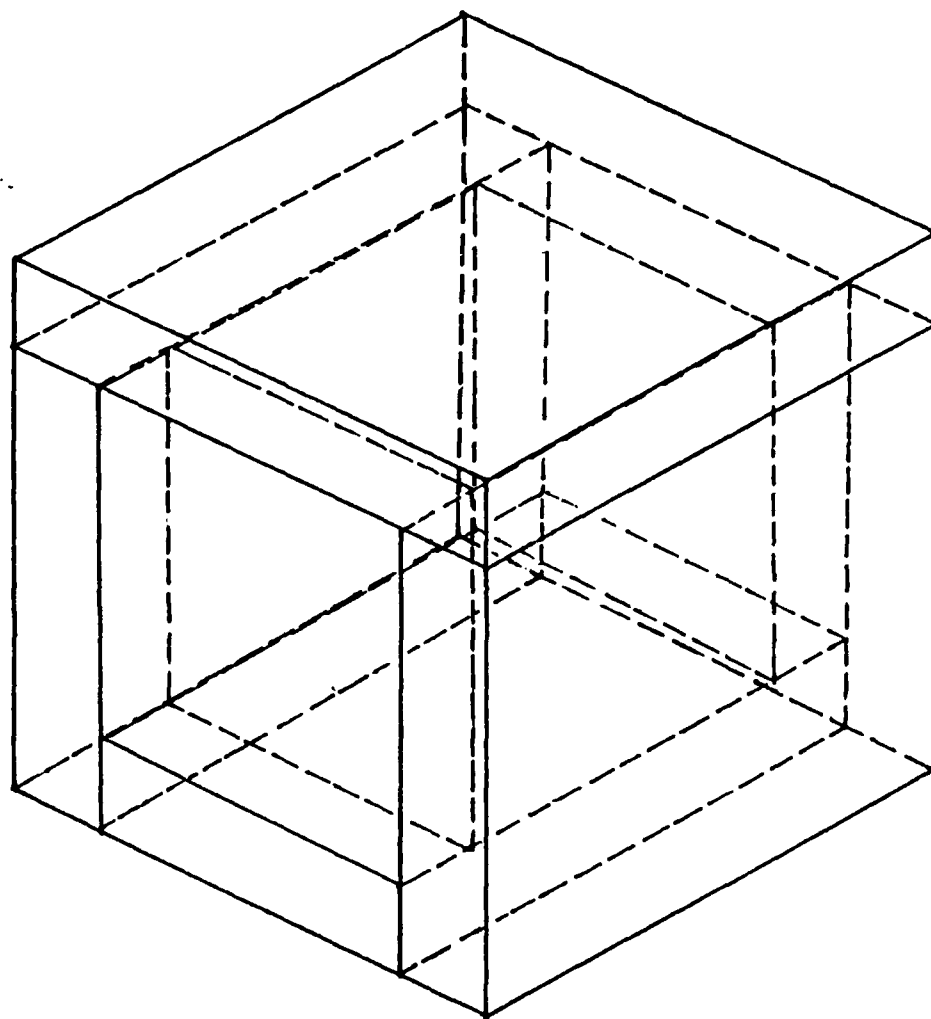


Figure 6. Isometric View

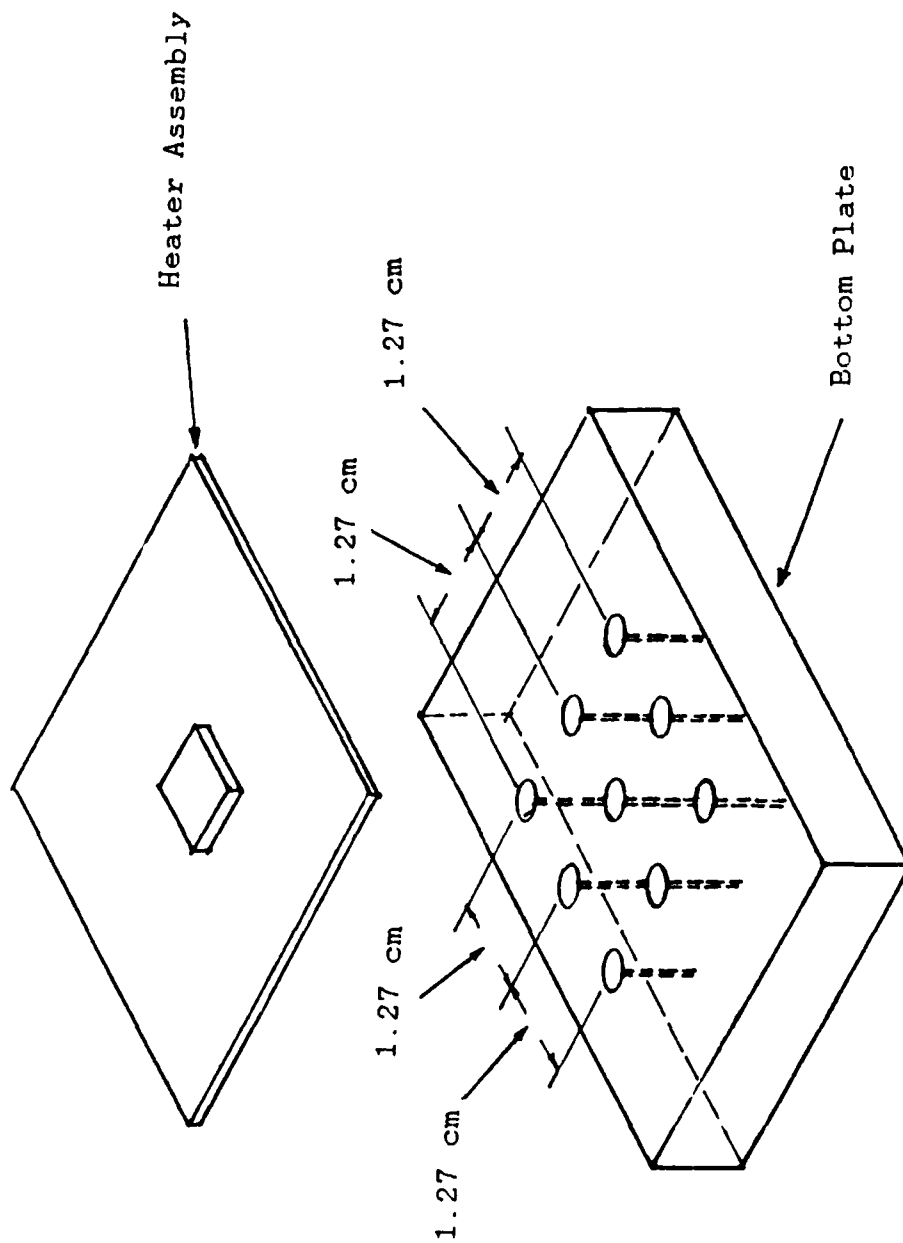


Figure 7. Bottom Plate/Heater Interface

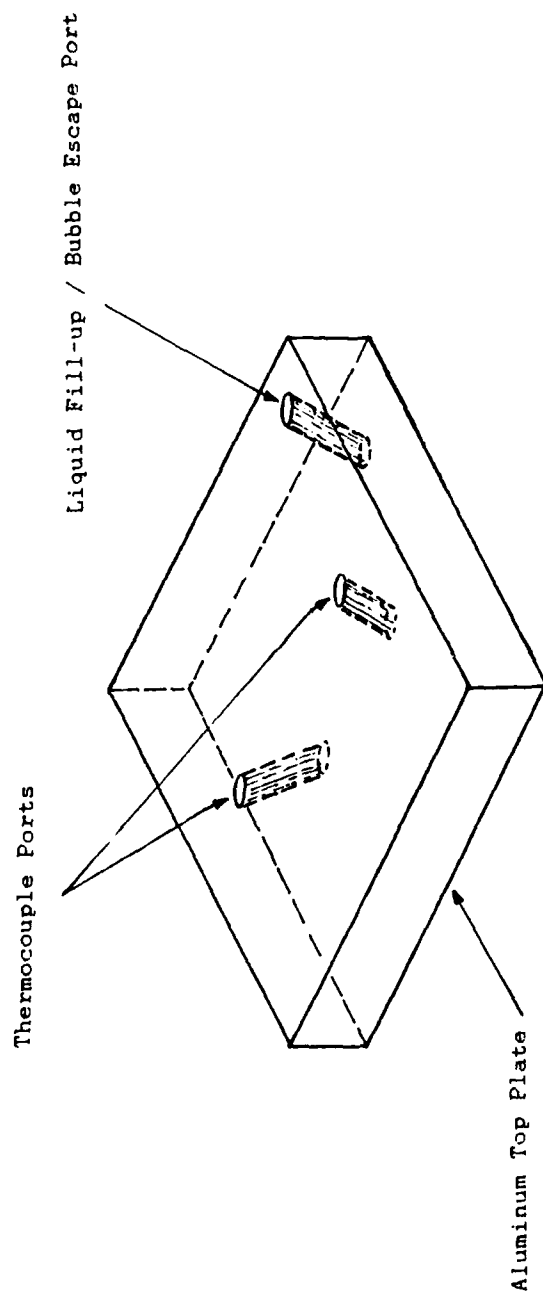


Figure 8. Immersion Cube Ports

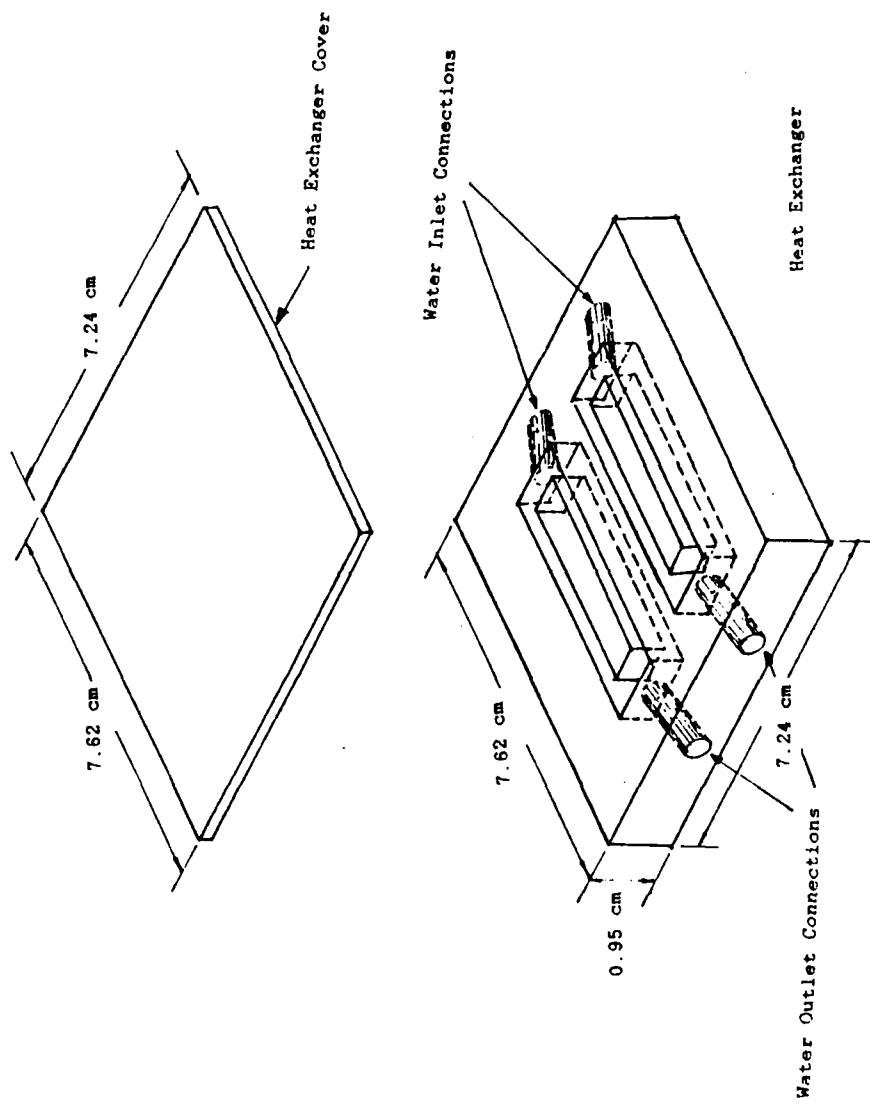


Figure 9. Heat Exchanger Assembly

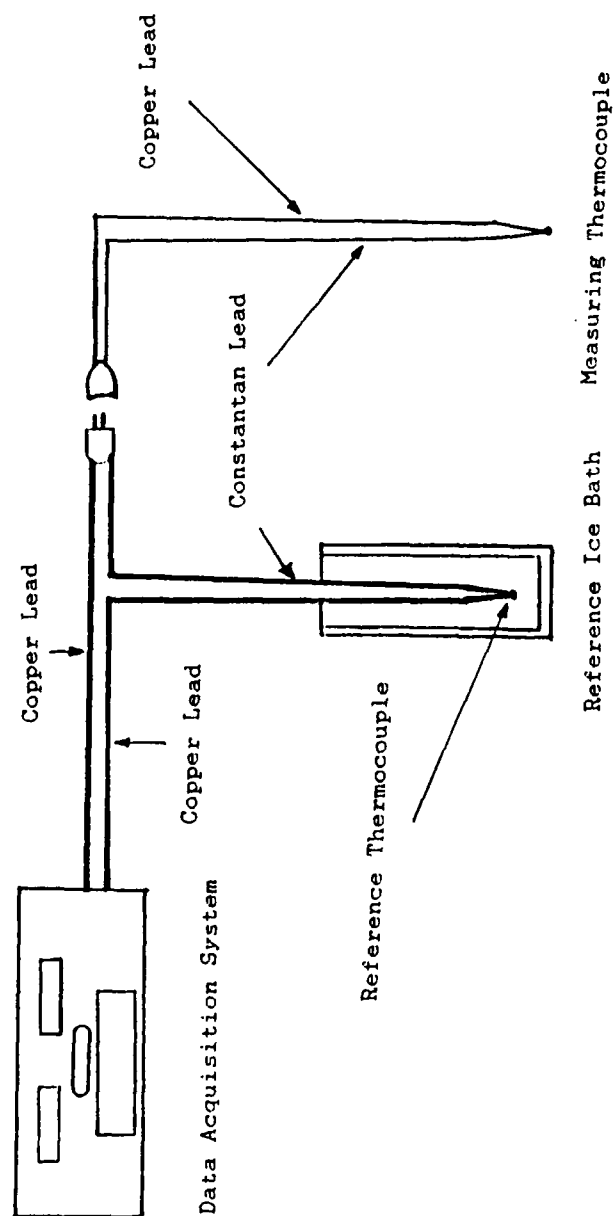


Figure 10. Reference/Sensing Thermocouple Connection

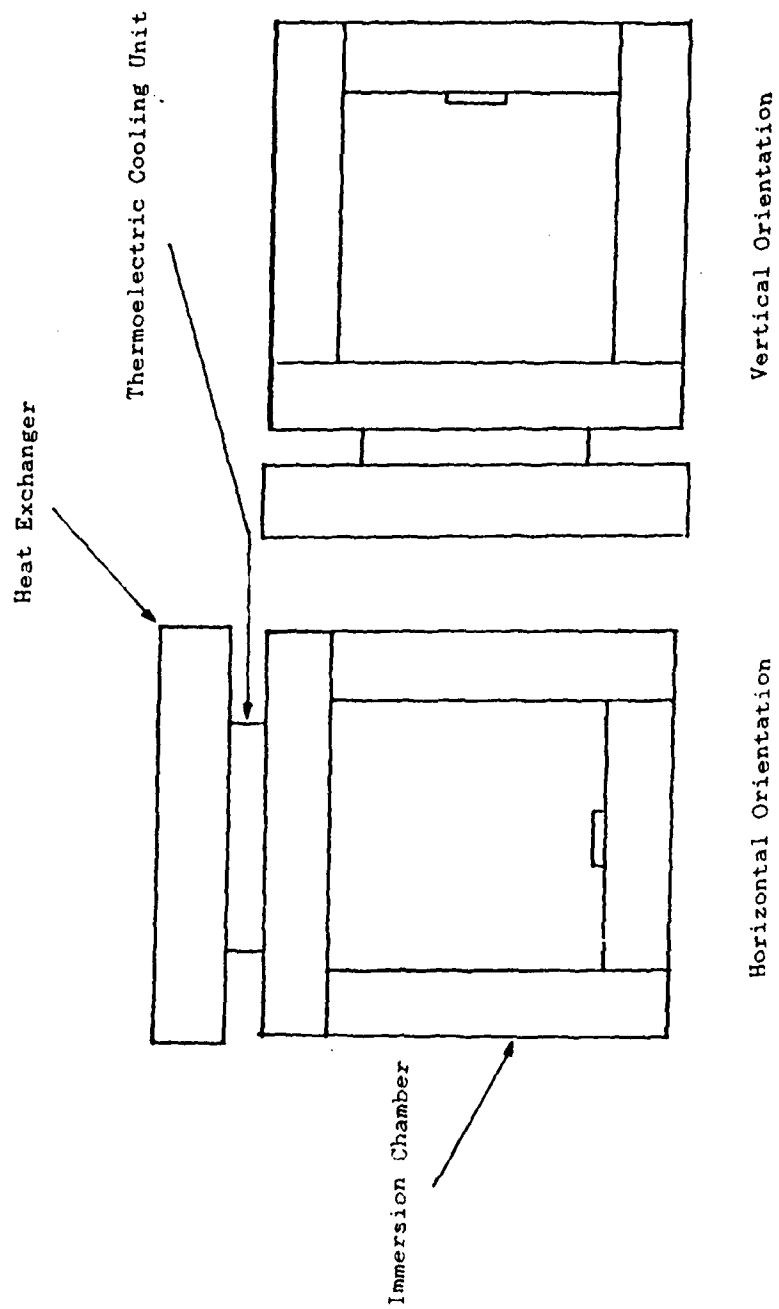


Figure 11. Chip Orientations

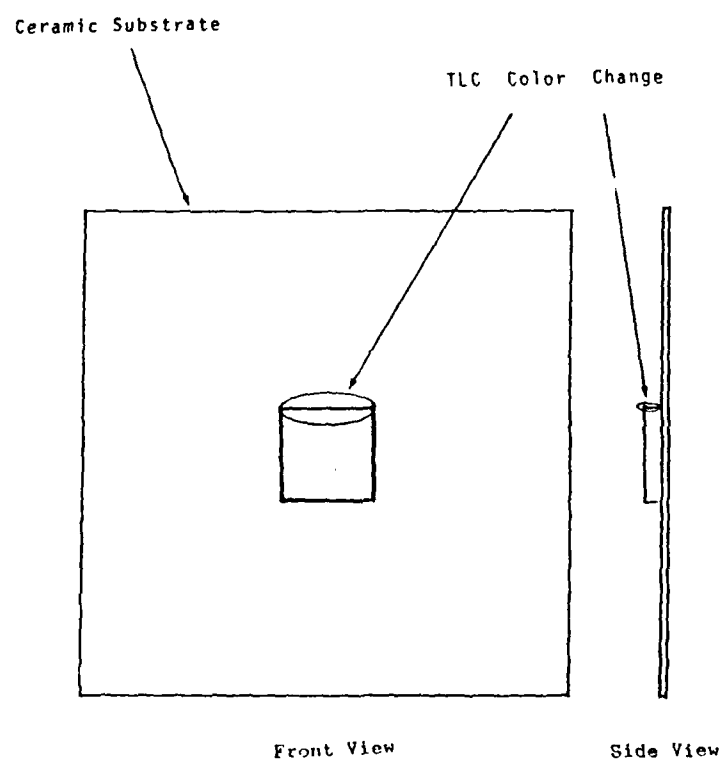


Figure 12. Vertical Orientation (Upper TLC Color Change)

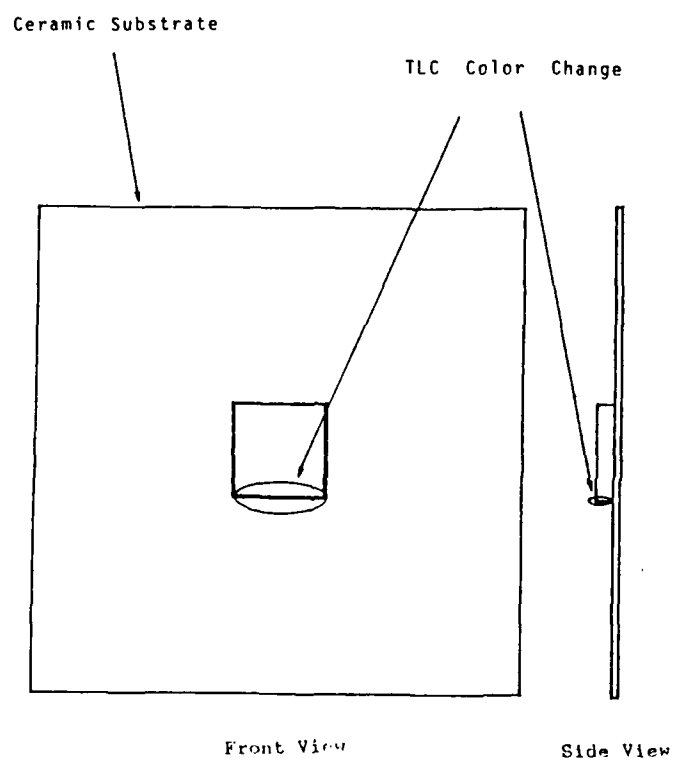


Figure 13. Vertical Orientation (Lower TLC Color Change)

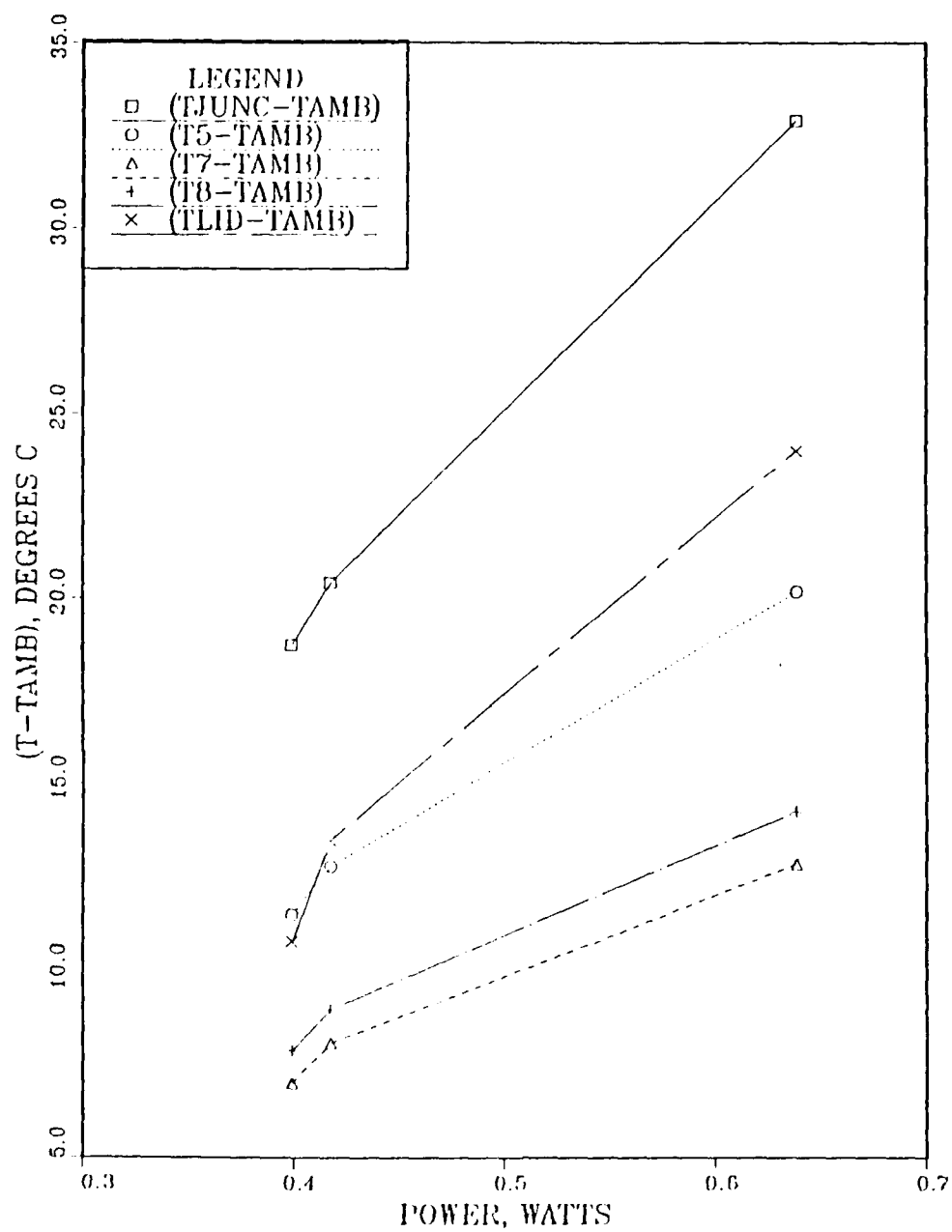


Figure 14. Heater Assembly Thermal Response in Air
(Horizontal Configuration)

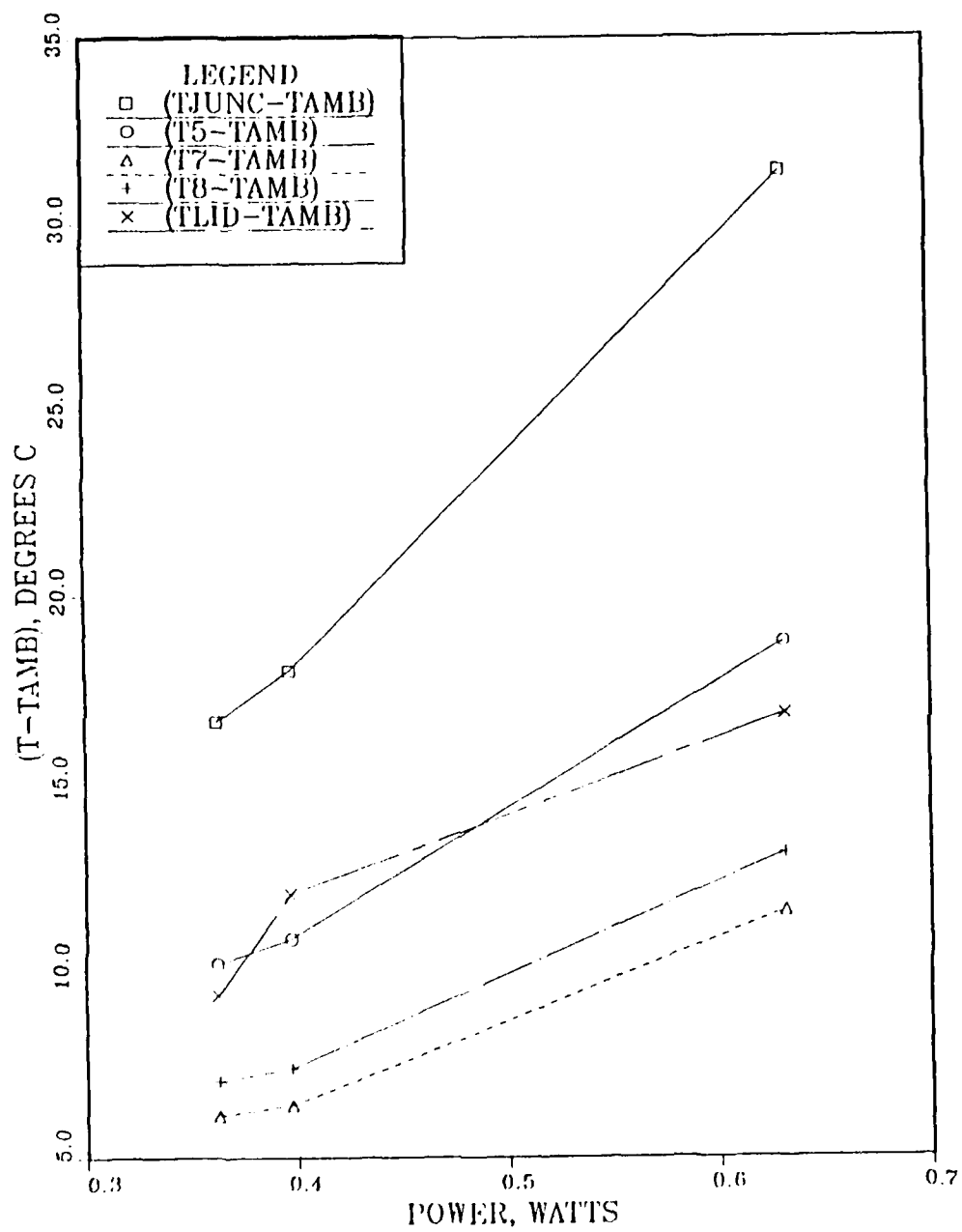


Figure 15. Heater Assembly Thermal Response in Air (Vertical Configuration)

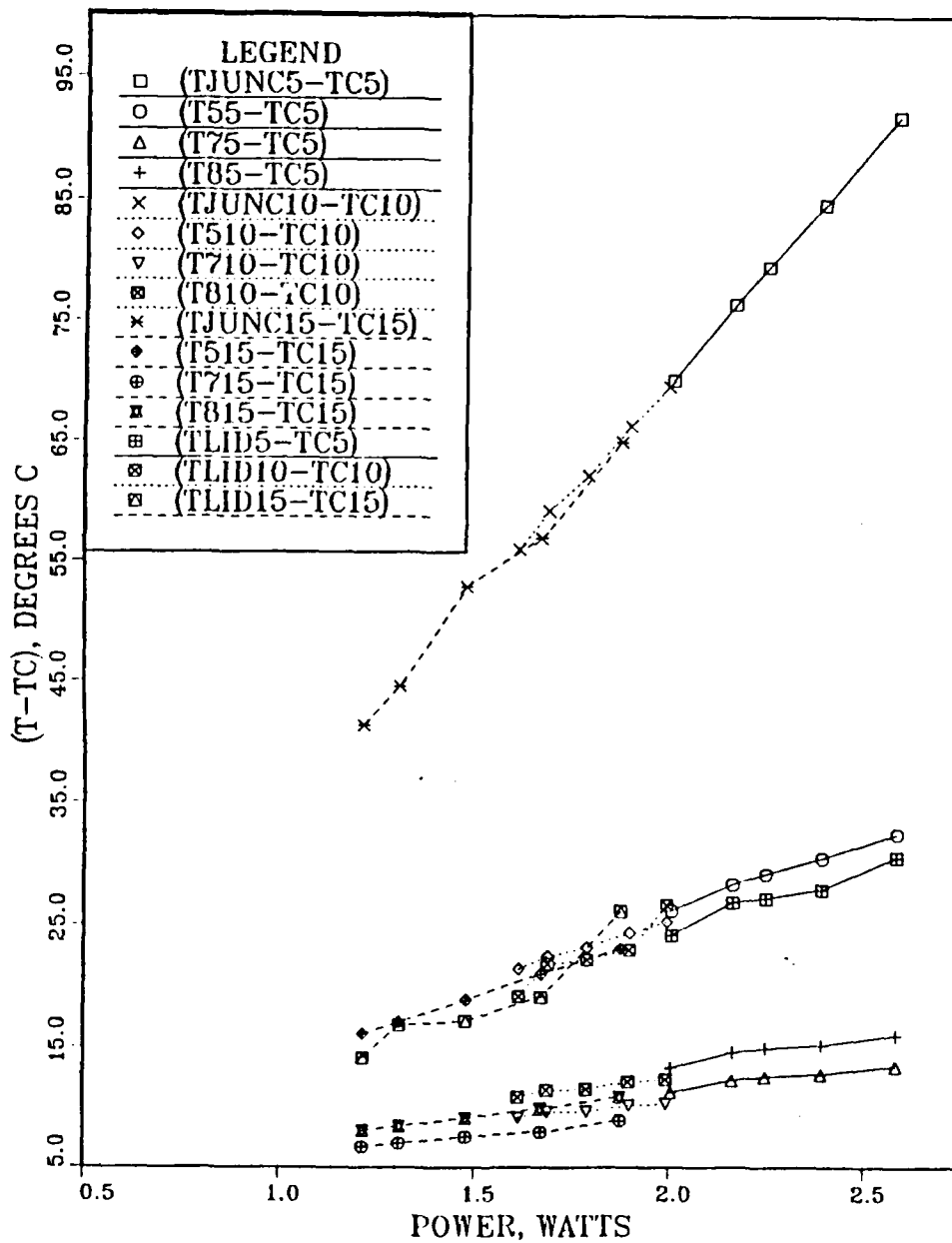


Figure 16. Heater Assembly Dimensional Thermal Response in FC-75 (Horizontal Configuration)

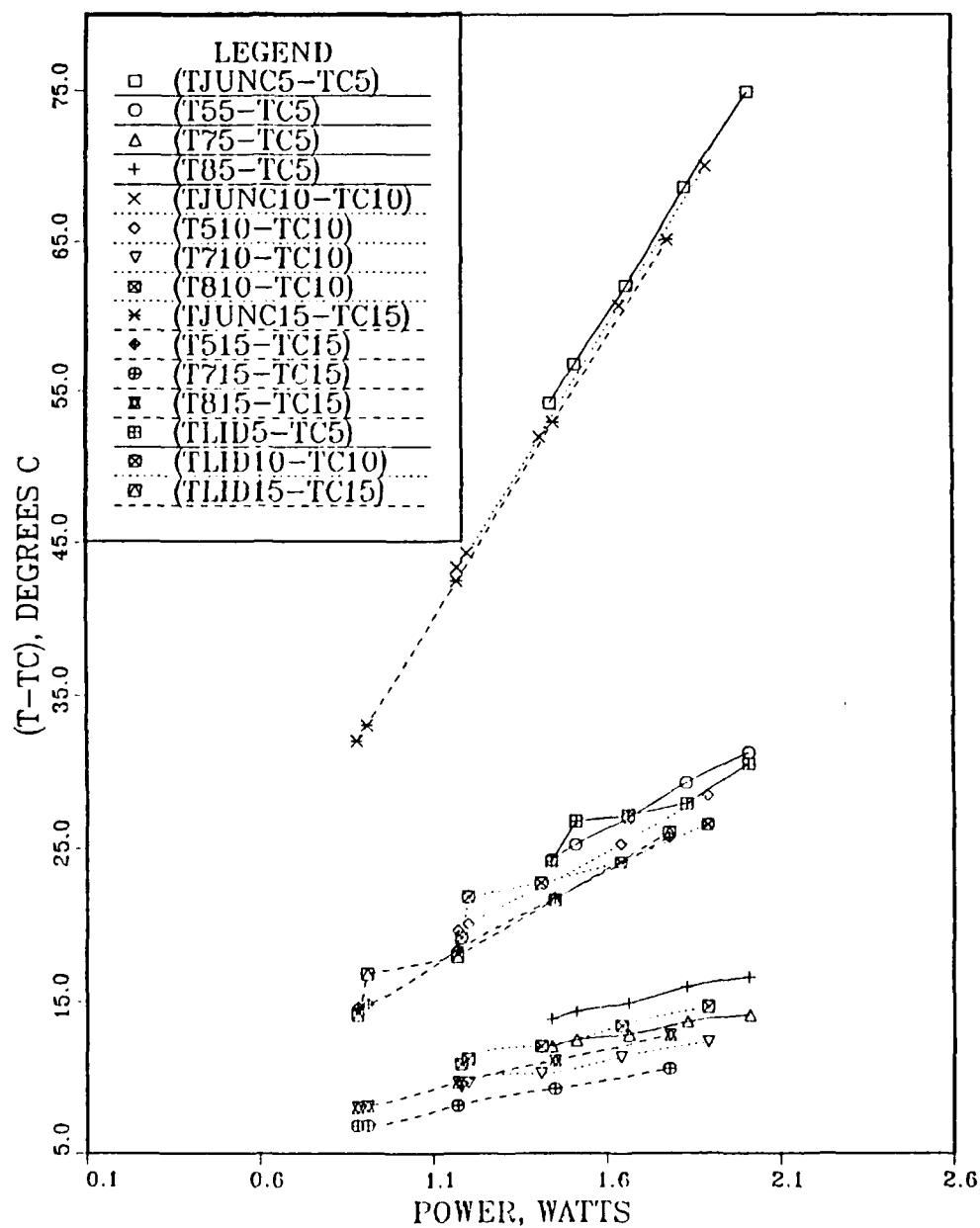


Figure 17. Heater Assembly Dimensional Thermal Response in FC-43 (Horizontal Configuration)

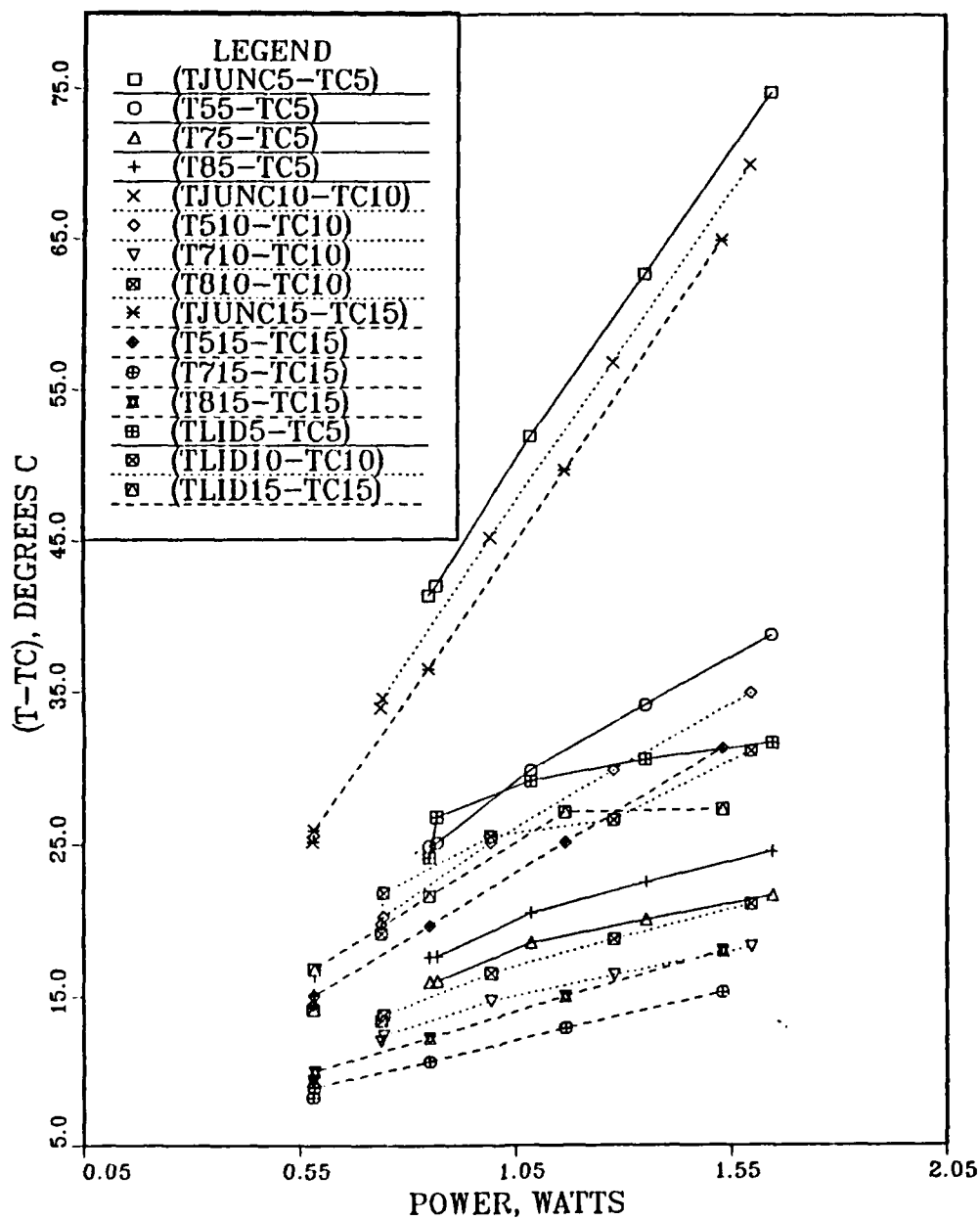


Figure 18. Heater Assembly Dimensional Thermal Response in FC-71 (Horizontal Configuration)

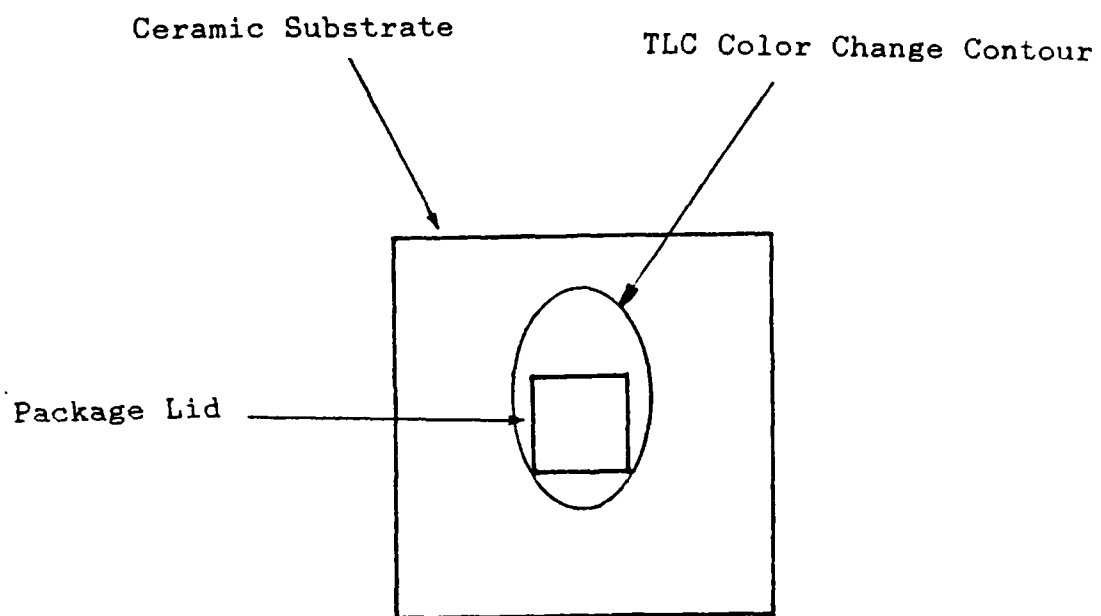


Figure 19. TCL Color Display in Vertical Configuration

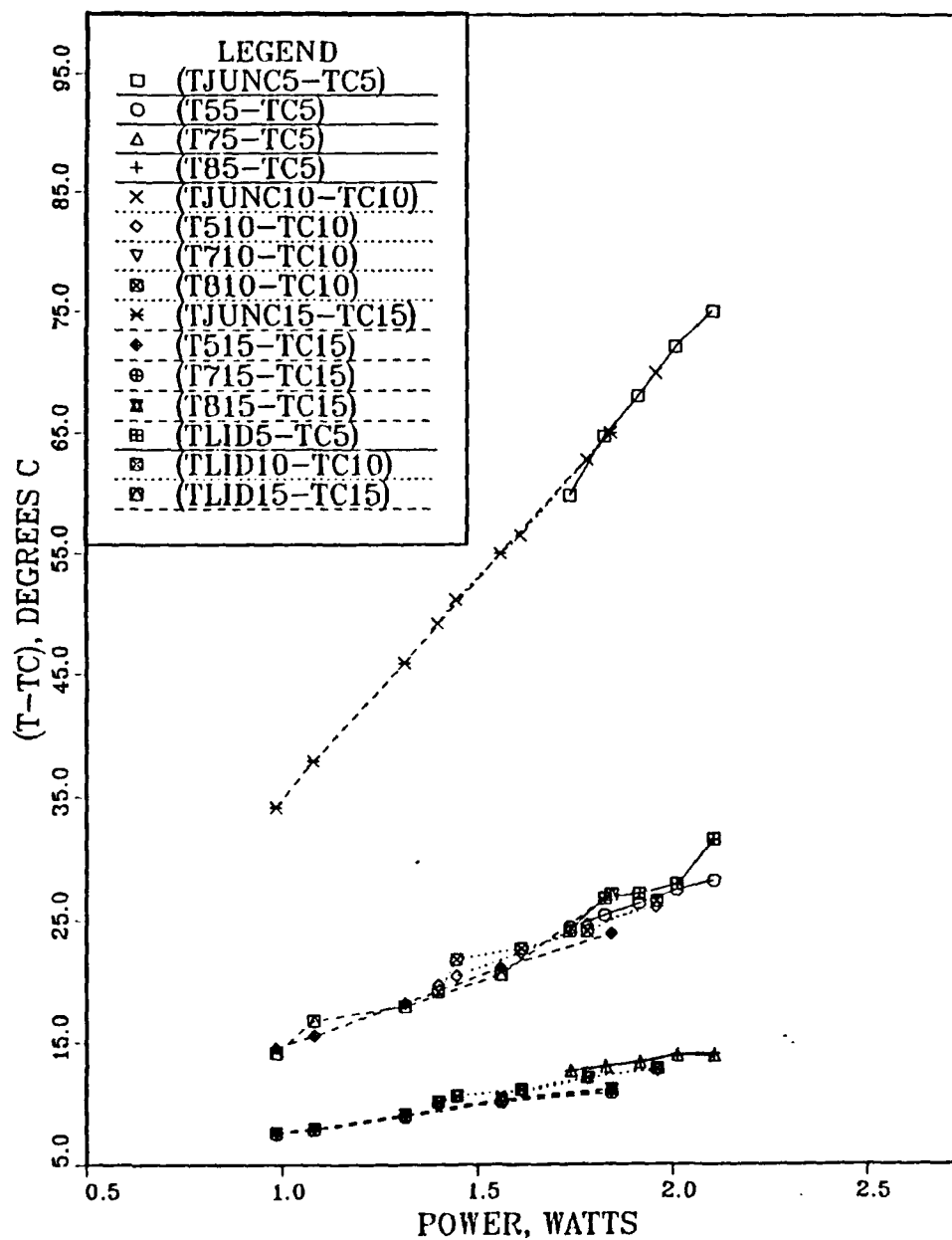


Figure 20. Heater Assembly Dimensional Thermal Response in FC-75 (Vertical Configuration)

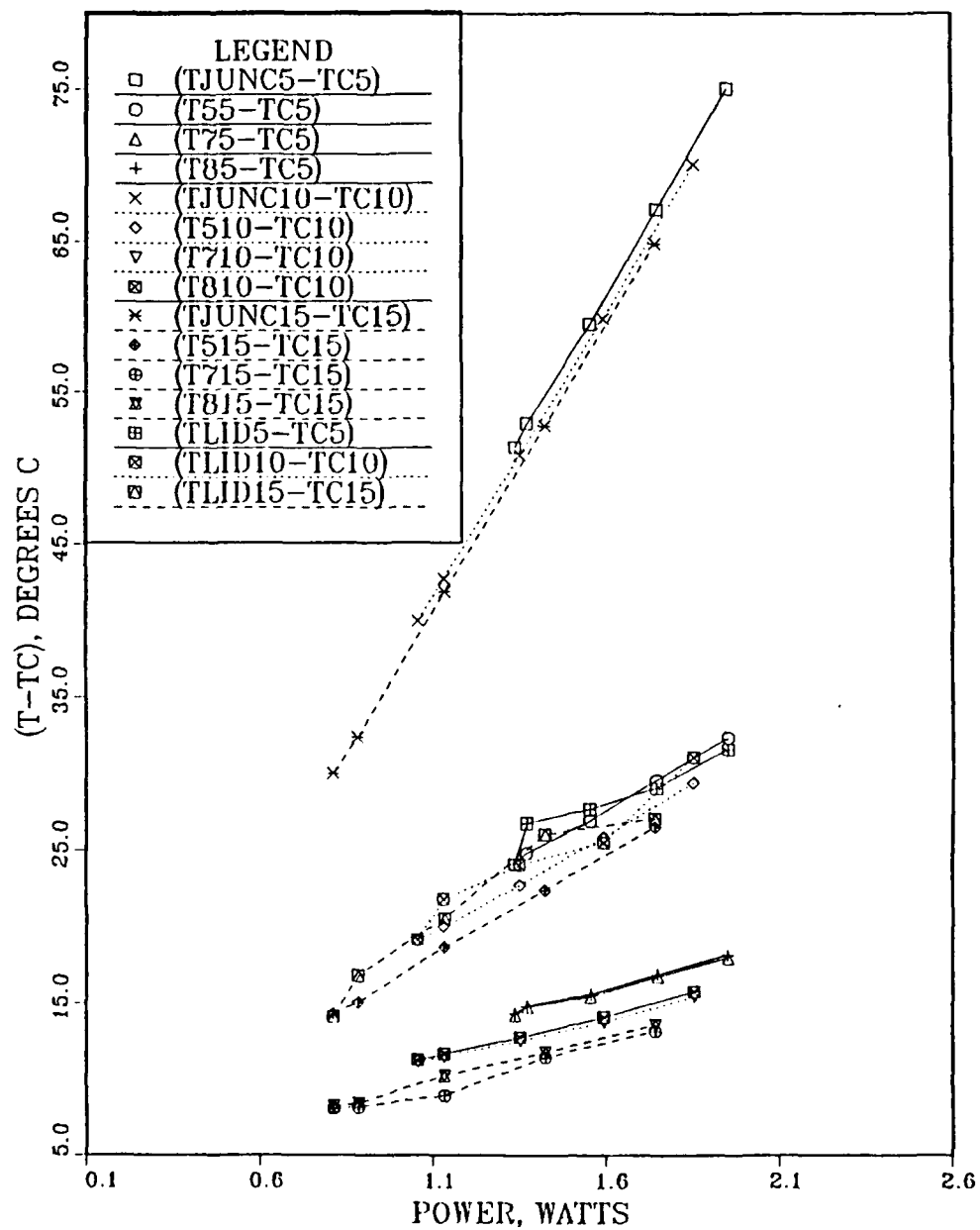


Figure 21. Heater Assembly Dimensional Thermal Response in FC-43 (Vertical Configuration)

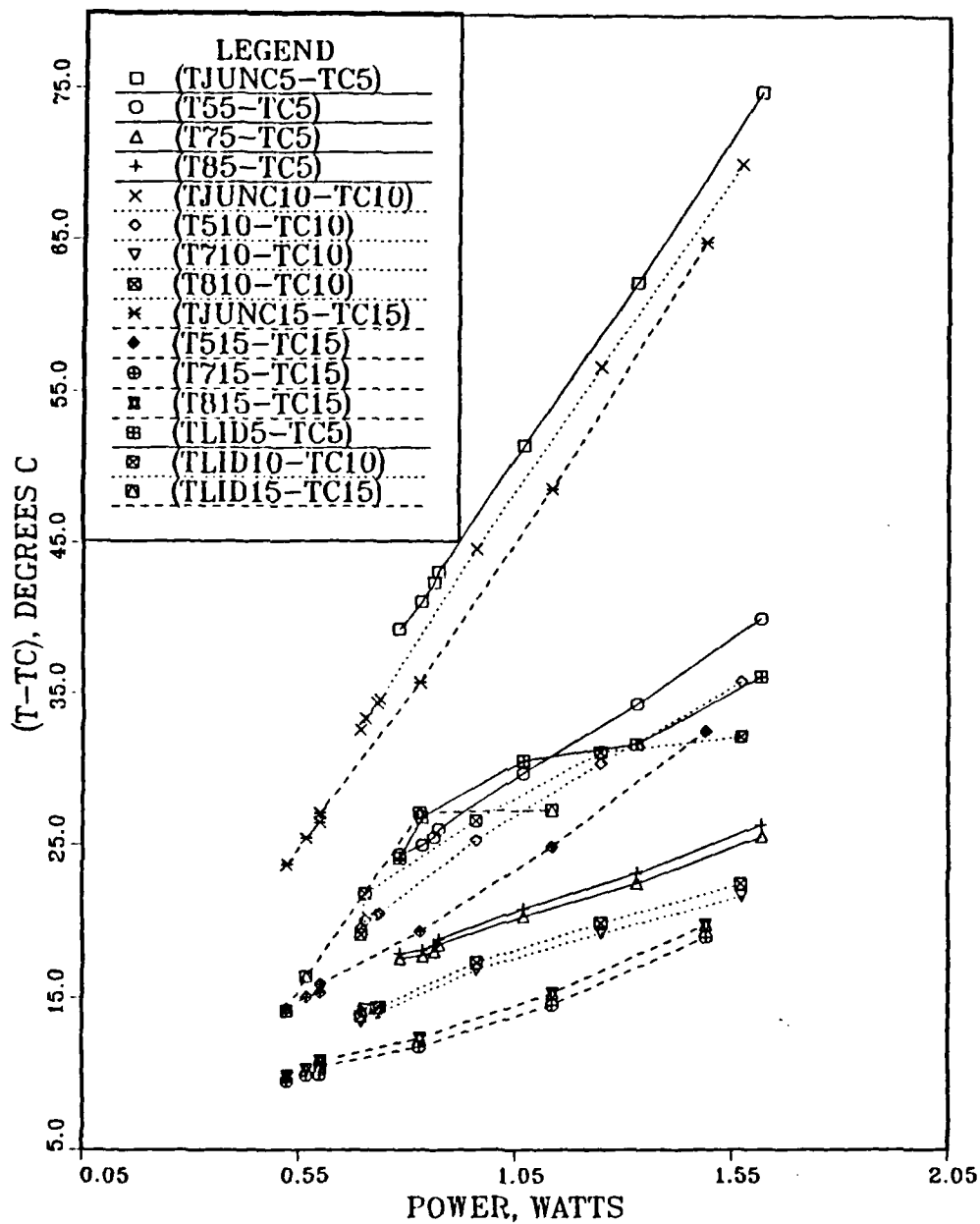


Figure 22. Heater Assembly Dimensional Thermal Response in FC-71 (Vertical Configuration)

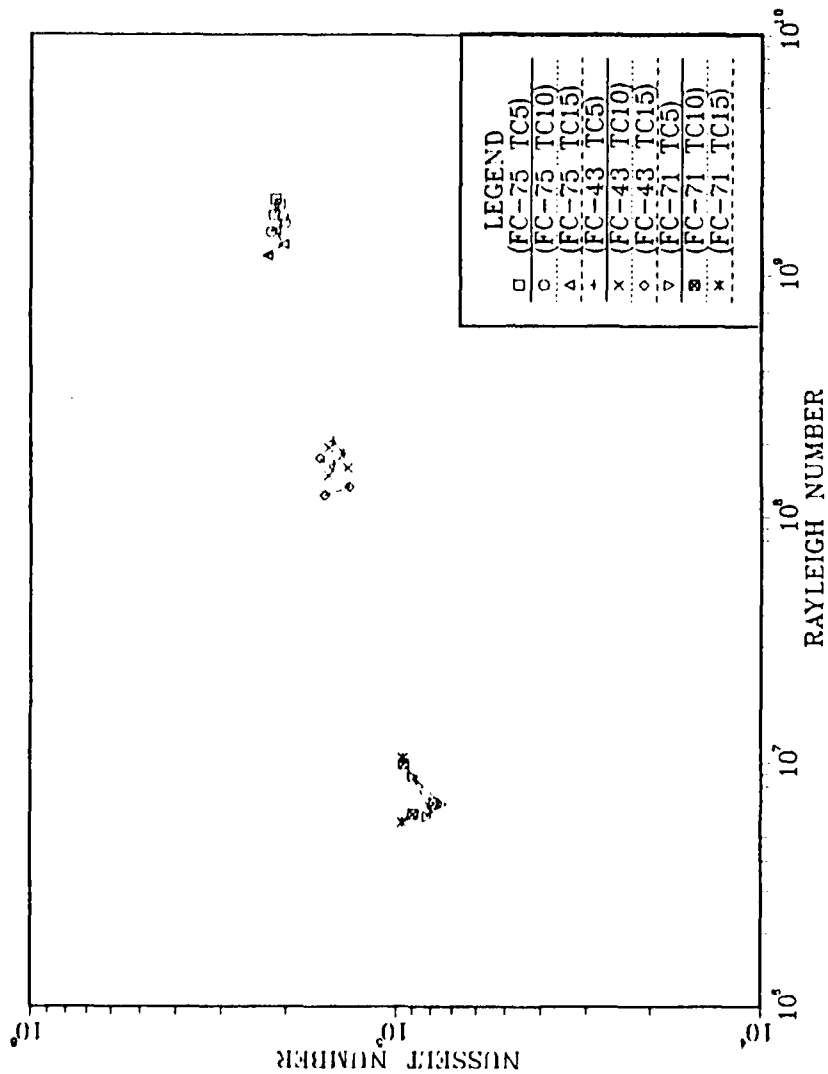


Figure 23. Heater Assembly Non-Dimensional Thermal Response in FC-75, FC-43 and FC-71 (Horizontal Configuration)

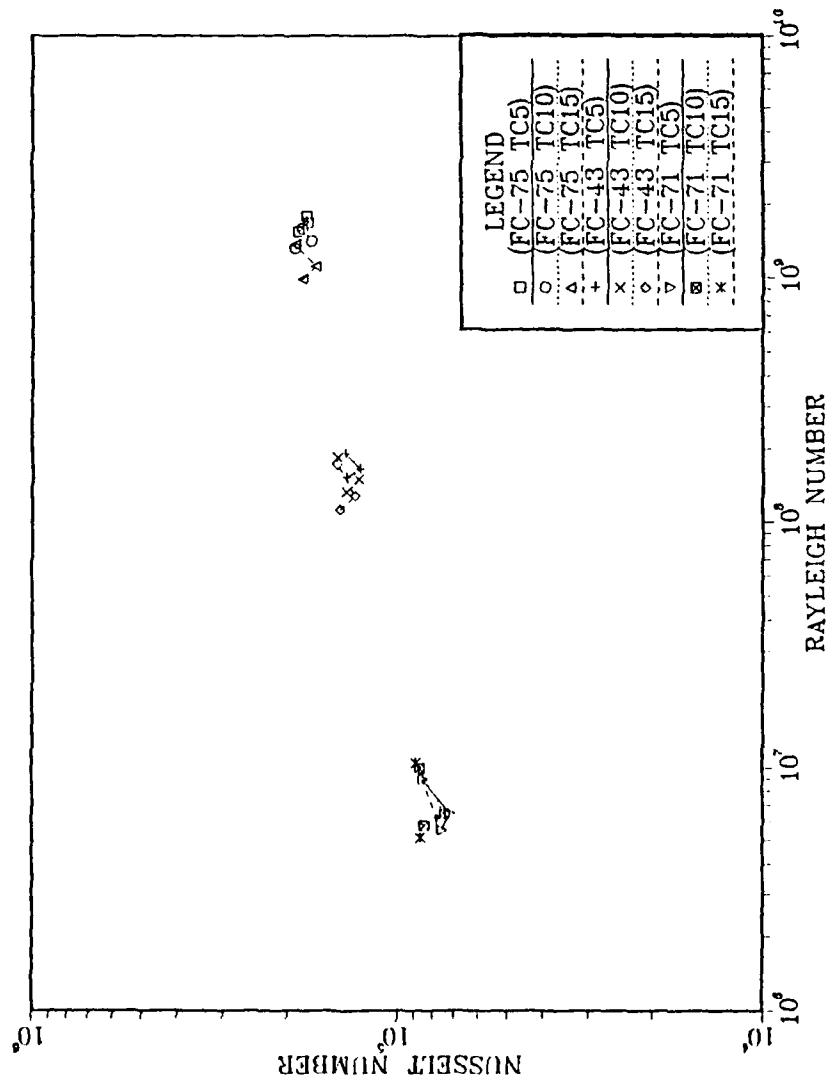


Figure 24. Heater Assembly Non-Dimensional Thermal Response in FC-75, FC-43 and FC-71 (Vertical Configuration)

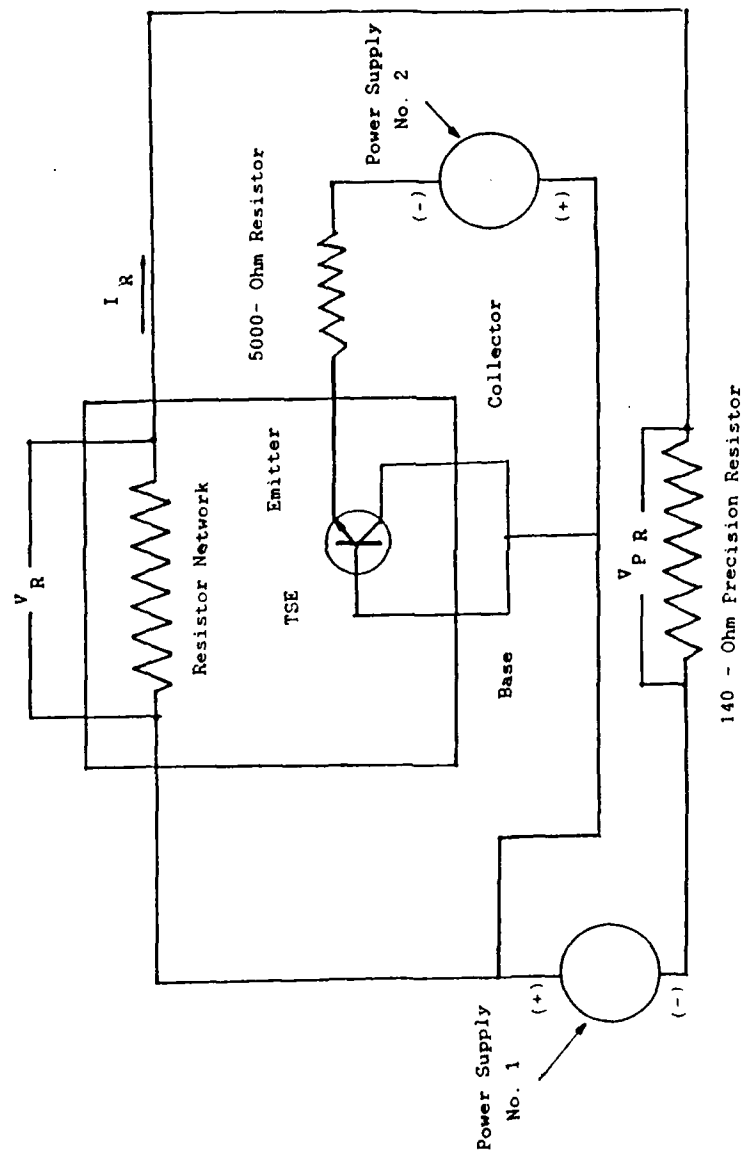


Figure 25. TI 1158 K-Factor Bar

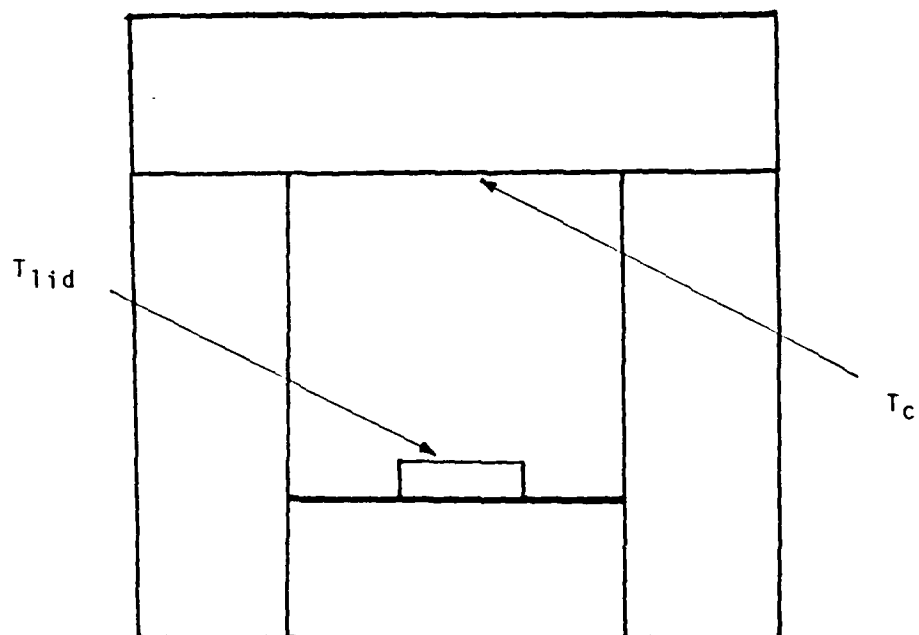


Figure 26. Film Temperature Determination

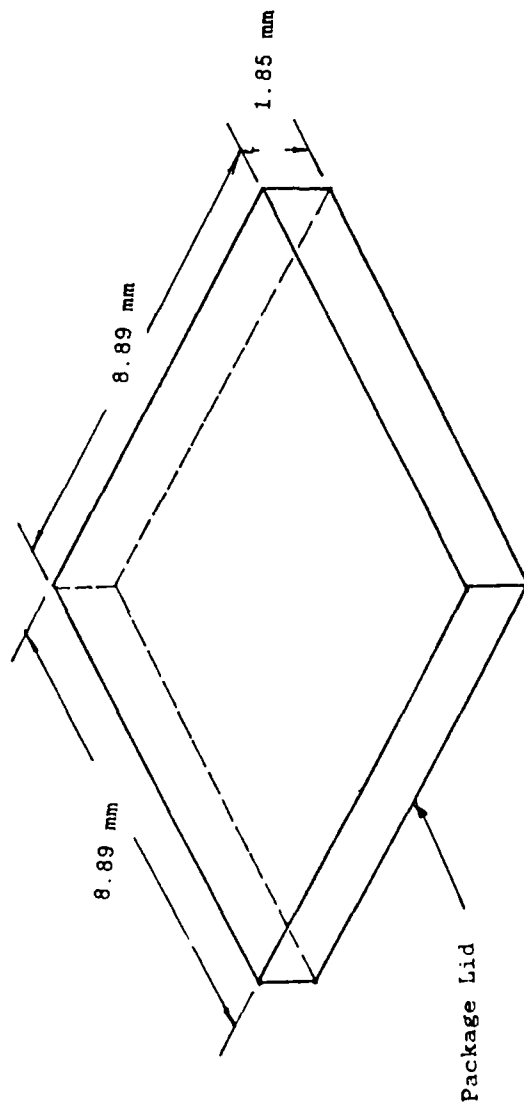


Figure 27. Lid Surface Area Determination

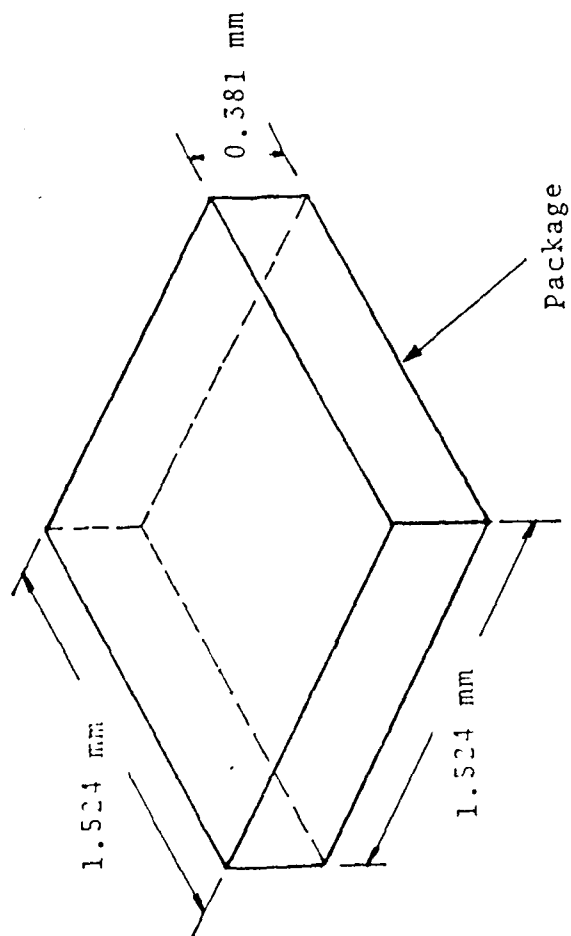


Figure 28. Package Volume Determination

LIST OF REFERENCES

1. Baker E., Liquid Cooling of Microelectronic Devices by Free and Forced Convection, Microelectronics and Reliability, v. 11, pp. 213-222, April 1973.
2. Baker, E., Liquid Immersion Cooling of Small Electronic Devices, Microelectronics and Reliability, v. 12, pp. 163-176, 1973.
3. Park, K. A. and Bergles, A.E., Natural convection Heat Transfer Characteristics of Simulated Microelectronic Chips, Transaction of the ASME, Journal of Heat Transfer, V. 109, pp. 90-96, February 1987.
4. Kelleher, M.D., Knock, R.H., and Yang, K.T., Laminar Natural Convection in a Rectangular Enclosure due to a Heated Protrusion on one Vertical Wall, part I: Experimental Investigation, Proc. 2nd ASME/JSME Thermal Engineering Joint Conference, Honolulu, Hawaii, pp. 169-177, 1987.
5. Lee, J.J., Liu, K.V., Yang, K.T., and Kelleher, M.D., Laminar Natural Convection in a Rectangular Enclosure due to a Heated Protrusion on one Vertical Wall, part II: Numerical simulations, Proc. 2nd ASME/JSME Thermal Engineering Joint Conference, Honolulu, Hawaii, pp. 179-185, 1987.
6. Liu, K.V., Yang, K.T., Wu, Y.W., and Kelleher, M.D., Local Oscillatory Surface Temperature Responses in Immersion Cooling of a Chip Array by Natural Convection in an Enclosure, Proc. of the Symposium on Heat and Mass Transfer in Honor of B.T. Chao, University of Illinois, Urbana- Champaign, pp. 309-330, October 1987.
7. Joshi, Y., Kelleher, M.D. and Benedict, T.J., Natural Convection Immersion Cooling of an Array of Simulated Electronic Components in an Enclosure Filled with Dielectric Fluid, Proc. of the International Symposium of Heat Transfer in Electronic and Microelectronic Equipment, Dubrovnik, Yugoslavia, 1988.

INITIAL DISTRIBUTION LIST

	No. of Copies
1. Defense Technical Information Center Cameron Station Alexandria, VA 22304-6145	2
2. Library, Code 0142 Naval Postgraduate School Monterey, CA 93943-5002	2
3. Professor Y. Joshi, Code 69JI Department of Mechanical Engineering Naval Postgraduate School Monterey, CA 93943-5002	2
4. Professor M.D. Kelleher, Code 69KK Department of Mechanical Engineering Naval Postgraduate School Monterey, CA 93943-5002	1
5. Department Chairman, Code 69 Department of Mechanical Engineering Naval Postgraduate School Monterey, CA 93943-5002	1
6. Mr. Alan Bosler Naval Weapons Support Center Code 6042 Crane, IN 47522	1
7. Mr. Duane Embree Naval Weapons Support Center Code 6042 Crane, IN 47522	1
8. Mr. Joseph Cipriano Executive Director Naval Sea Systems Command Washington, D.C. 20362-5101	1

- | | | |
|-----|--|---|
| 9. | Naval Engineering Curricular Office
Code 34
Department of Mechanical Engineering
Naval Postgraduate School
Monterey, CA 93943-5004 | 1 |
| 10. | LT. Rufino A. Paje
4382 Hydrangea Ct.
San Diego, CA 92154 | 1 |
| 11. | Dean
Institute of Technology
Far Eastern University
Nicanor Reyes Ave.
Sampaloc, Manila,
Philippines 2806 | 1 |
| 12. | National Science Development Board
C/O Dean
Institute of Technology
Far Eastern University
Nicanor Reyes Ave.
Sampaloc, Manila,
Philippines 2806 | 1 |